CHARACTERIZATION OF MICROPLASTICS IN THE WATER COLUMN OF WESTERN LAKE SUPERIOR

A THESIS
SUBMITTED TO THE FACULTY OF THE
UNIVERSITY OF MINNESOTA
BY

JOHN MCGRANE FOX

IN PARTIAL FULFILLMENT OF THE REQUIREMENTS
FOR THE DEGREE OF
MASTER OF SCIENCE

DR. MELISSA MAURER-JONES, ADVISOR

AUGUST 2021

Abstract

The amount of plastic waste in the natural environment has increased precipitously over the past 60 years and plastic contamination is now ubiquitous in aquatic systems across the planet. Microplastic represents a particularly pernicious form of plastic pollution as it is impossible to practically remediate owing to its size and already extensive distribution throughout the environment. While the reality of microplastic in the Laurentian Great Lakes has received substantial scientific attention, more work is required to fully characterize its behavior and fate in this unique freshwater system. At present, very little is known regarding the vertical distribution of microplastics throughout the water column. Most sampling campaigns in the Great Lakes have to this point focused on surface waters, sediments, and shorelines, leaving the water column conspicuously under sampled and undiscussed in the literature. In this research, we characterized the vertical distribution of microplastics in the water column of Western Lake Superior. We hypothesize the chlorophyll maximum to have the largest abundance of microplastics because it coincides with the depth of the pycnocline where the change in water density may allow trapping of microplastics that become too dense to float yet are not dense enough to reach benthic sediments. To achieve this work, we compared several novel methods for collecting microplastic samples from the water column, including Niskin bottle volume-sampling, in situ pumping, and serial filtration in a custom-built filter tower. In this research, we found evidence that in strongly stratified water columns, microplastic particles aggregate at the depth of the chlorophyll maximum, although this aggregation was not observed at sites with well-mixed water columns. Additionally, subsurface waters tended to have the highest abundance of microplastic particles indicating that buoyant microplastics are likely to preferentially accumulate in surface waters. Beyond characterization of the water column, this thesis work also sought to build a completely automated analytical pipeline for the bias-free characterization and quantification of microplastic particles in natural samples. To this end, a program was developed to count and detect microplastic particles based on two-dimensional spectral data obtained using an FTIR microscope. Computational analysis of the data yielded microplastic counts on the same order of magnitude as the manual analysis and yielded very similar trends. Overall, this research is an important first step towards a better

understanding of the distribution of microplastics in the water column of Lake Superior and demonstrated an analytical approach for the bias-free detection of microplastics in natural samples using FTIR microscopy.

Table of Contents

List of Tables

List of Figures

List of Abbreviations

ATR	Attenuated Total Reflectance
BNL	Benthic Nepheloid Layer
CTD	Conductivity Temperature Depth
DLS	Dynamic Light Scattering
EDS	Energy Dispersive X-ray Spectroscopy
FPA	Focal Plane Array
FTIR	Fourier Transform Infrared Spectroscopy
GC	Gas Chromatography
IR	Infrared
LCCMR	Legislative-Citizen Commission on Minnesota Resources
MALS	Multi Angle Light Scattering
MCE	Mixed Cellulose Ester
MP	Microplastic
MS	Mass Spectroscopy
NP	Nanoplastic
PE	Polyethylene
PET	Polyethylene Terephthalate
PLA	Polylactic Acid
PP	Polypropylene
PS	Polystyrene
PTFE	Polytetrafluoroethylene
PVC	Polyvinylchloride
SEM	Scanning Electron Microscopy
TEM	Transmission Electron Microscopy
UV	Ultraviolet
WLSSD	Western Lake Superior Sanitary District
WM	Western Mooring
WWTP	Wastewater Treatment Plant

CHAPTER 1. INTRODUCTION

1.1 Background

Global plastic production has steadily increased since the 1950s when plastic initially became widely available in the developed world. Plastics are now so commonplace in daily life that it is rare when humans are neither in contact with plastic textile fibers nor actively using plastic products in some way. It is estimated that between 1950 and 2015, net global plastic production was 8300 megatonnes including 1000 megatonnes of additives.[1] In 2016, total plastic production was 393 megatonnes.[2] In 2008, approximately 4% of extracted fossil fuels were used for plastic production and by 2050, it is estimated that plastic manufacturing and processing could account for 20% of global fossil fuel consumption due to the disproportionately large growth in demand for plastic.[2]

The ubiquity of plastic can largely be attributed to the fact that it is a low-cost, high-performance material. The physicochemical properties of plastics are such that they can be endlessly customized to suit both very broad and very specific end uses. Plastic polymers are highly desirable materials as they are durable, malleable, moldable, hydrophobic, lightweight, bio-inert, and are excellent thermal and electrical insulators. Prior to the advent of plastics, the properties of common building and manufacturing materials were predominantly available only in discrete increments. For example, wood is available in many discrete increments of hardness depending on the species of tree. However, if a material with an intermediate hardness is required for a certain application, wood cannot satisfy that requirement. Plastic is unique in that the available possibilities for physicochemical properties constitute a continuum. Between the possible physical limits for polymers, properties may be engineered such that any value on the bounded continuum is achievable.[2] Furthermore, additives such as plasticizers, antioxidants, and UV stabilizers can also be included to increase durability and resist degradation, among other desirable physical property modifications.[3]

1.2 Plastic Waste in the Environment

The customizability of polymers has rendered them indispensable to both the packaging and construction industries, the two largest end uses for plastic globally.[2] Indeed, plastic packaging alone accounts for 39-42% of resin use, or approximately 146 megatonnes of plastic production in 2015.[1,2,4] Due to the inherent brevity of the service life of plastic packaging, the vast majority of plastic packaging is discarded within one year of production and therefore represents a major source of plastic waste.[1] Of all plastics produced between 1950 and 2015, it is estimated that only 30% are still in use. Of the remainder, 12% has been incinerated, 9% has been recycled (only 10% of which has then been re-recycled), and 79% has been discarded to landfills and the environment, a portion equal to 4900 megatonnes as of 2015 (Figure 1).[1] Although recycling rates have increased in recent years, in 2019 recycled plastics only met 10% of global demand for plastics.[5] As of 2014, some regions such as China and Europe had achieved plastic recycling rates of 25% and 30%, respectively, whereas in 2019 the plastic recycling rate in the US was comparatively low at 9.4%.[2]

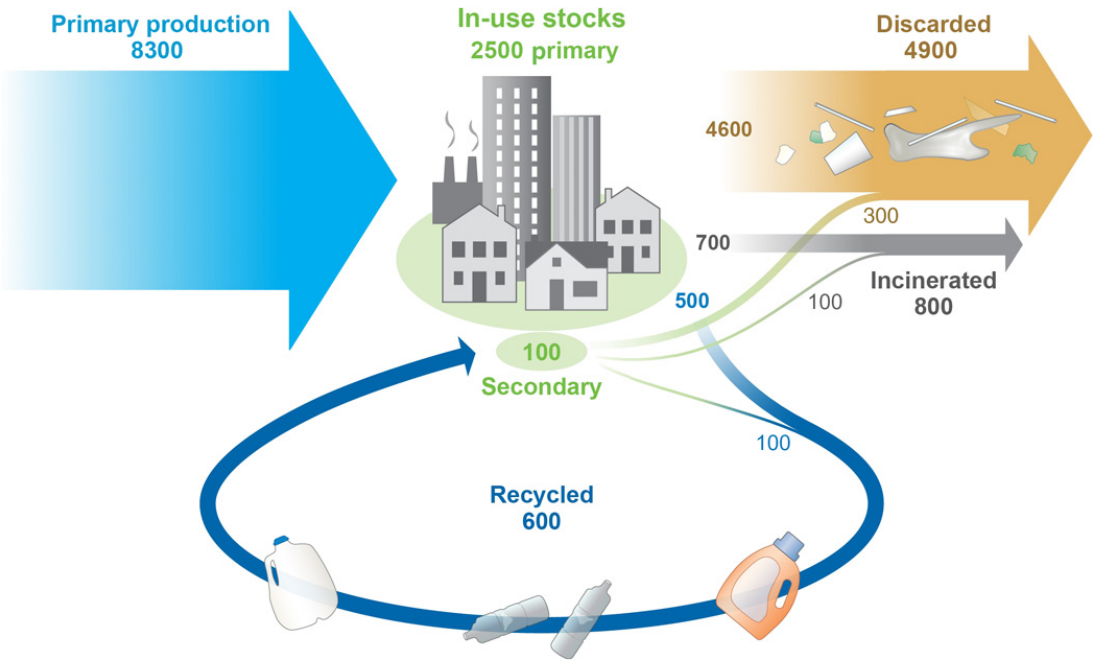

Figure 1. Plastic fate, 1950 to 2015, in megatonnes.[1]

Plastic that is neither incinerated nor recycled can either be properly managed in a waste stream or mismanaged.[6] Because plastic is very resistant to degradation in the natural environment and can potentially persist for hundreds of years or even millennia, depending on the polymer, proper management of plastic waste means long-term placement in a contained landfill that prevents plastic escaping to the natural environment.[6,7] All plastic waste that is not placed in controlled landfills is classified as mismanaged and is amenable to subsequent dispersion throughout the natural environment.[6] In 2010, it was estimated that 99.5 megatonnes of plastic waste was generated by communities within 50 km of the world's oceans and seas. Of this waste, 31.9 megatonnes was mismanaged with 4.8 - 12.7 megatonnes of the mismanaged fraction entering the ocean, although *in situ* assays of total plastic in ocean surface waters are several orders of magnitude lower at 1.1 – 269 kilotonnes.[6] This discrepancy is due to the challenge of accurately sampling and quantifying plastic waste in aquatic environments.[8,9,10,11] More fundamentally, the gulf between the amount of plastic known to enter aquatic environments and the amount sampled from those environments is due to vastly incomplete knowledge regarding the behavior, fate, and ultimate sink of plastic waste in aquatic environments.[8,12]

Mismanaged plastic waste can enter the natural environment and marine and freshwater systems in a number of ways. Plastic waste can be deposited directly to the environment as litter or carried into the environment from landfills via storm water runoff and wastewater treatment plants (WWTPs) via effluent.[13] Another way that plastics enter the environment is through the degradation of everyday plastic materials (i.e. rubber tires, synthetic fabrics, maritime equipment, polymer coatings, etc.), which then fracture and are carried throughout the environment.[14] Larger fragments may remain closer to where they were originally shed whereas smaller fragments may be entrained in wind and water leading to widespread dispersal throughout the environment.

Once in the aquatic environment, plastic waste may undergo a variety of physical and chemical transformations. Together, these transformations are typically referred to as weathering and include photochemical degradation, photothermal degradation, mechanical abrasion, hydrolysis, and biodegradation.[15,16] The magnitude of each of these transformations depends on the environment in which the weathering occurs and also on

the specific properties of the polymer that is being degraded.[17] Photooxidation and photothermal oxidation will be greatest in environments with high insolation and high temperatures, respectively.[18,19] Mechanical abrasion will be greatest in environments where plastics are subjected to shearing forces such as in flowing water or in bodies of water with significant wave action.[15] Hydrolysis of plastic waste will be enhanced under either acidic or basic conditions and is therefore dependent on water chemistry.[17] Biodegradation of plastic waste typically occurs after the preceding abiotic degradation processes and is contingent upon the presence of polymer degrading microorganisms.[20] Overall, the weathering of plastics in aquatic environments proceeds via many complex and interacting transformations that have yet to be fully characterized. Accordingly, weathering is currently poorly understood.[16] Nonetheless, the net result of weathering is known to be a decrease in the size of plastic waste fragments and an increase in the number of plastic particles.[16]

1.3 Classifications

The weathering and concomitant decrease in size of plastic waste in aquatic systems has led to the current global situation wherein a vast proportion of aquatic plastic waste is microscopic in size. In order to differentiate this portion of microscopic plastic waste from larger macroscopic plastic waste (macroplastic), the term “microplastic” was coined in 2004 by Thompson *et al.*[21] Since that time, and as more scientific attention has been turned toward the microplastic (MP) conundrum, both operational and objective definitions for the term “microplastic” have been put forward.[22] The majority of these definitions use the largest dimension of a plastic particle as the determinant characteristic of a MP and define a MP as a plastic particle whose greatest dimension does not exceed 5 mm.[23] Another definition uses the smallest dimension of a plastic particle as the determinant characteristic, such than any plastic particle or fragment with a single dimension smaller than 5 mm is considered a MP.[24] Under this definition, any polymer film with a thickness less than 5 mm is classified as a microplastic, regardless of the two-dimensional area of the film. Although the former of these two definitions is the most widely employed definition as it is intuitive and unambiguous, it is oftentimes expressed

ambiguously in the literature. That is, much of the literature defines MPs simply as any plastic fragment smaller than 5 mm.[23] Although this definition *implies* that all dimensions of a plastic particle must be less than 5 mm in order to qualify as a MP, oftentimes this is not explicitly stated, so the intuitive definition is rendered ambiguous by the mere existence of the alternative definitive scheme. Plastic morphology further complicates such seemingly simple definitions. In particular, the classification of plastic fibers should be explicitly addressed in any definition. While plastic fibers are inherently smaller than 5 mm in diameter, fiber length may exceed 5 mm and therefore any thorough definition should address whether fibers longer than 5 mm are still considered MPs.

Even though MP definitions do not technically include a lower size limit, when operationally defined there is a lower size limit as determined by the method of sampling.[25] For example, when MP samples are collected with a 333 μm mesh net, the lower size limit for MPs will be operationally defined as 333 μm because any particle below this threshold will not be collected.[23,25,26] Clearly then, in order to promote the facile comparison of results in the field of MP research, definitions must be stated unambiguously. In any given study, what a MP is, and what it is not, should be equally and abundantly clear.

Recently, attention has been drawn to plastic waste of an even smaller dimension, a fraction that is now being referred to as nanoplastic (NP). Similar to MPs, there is as yet no universally agreed upon definition regarding the dimensions for NP particles. The upper size limit for NPs has been alternately proposed as 1000 nm (1 μm) and 100 nm.[16,27,28] An upper size limit of 1000 nm is cited as intuitive from a nomenclature point of view and conforming to existing definitions for nanomaterials, whereas an upper size limit of 100 nm is cited as being representative of the scale whereat NPs exhibit physicochemical properties unique to the nanoscale (i.e. Brownian motion and localized surface plasmons) and not observed in larger particles of the same material.[29,30,31] In many ways, NP can be thought of as occupying the size range between particulate plastic and molecular plastic.

To make the morass of classification even more confusing, some studies have used additional terms such as submicro-plastic (between NP and MP) and mesoplastic (between MP and macroplastic) to refer to intermediate size ranges of plastic

particles.[32,29] A 2019 literature summary by Hartmann *et al.* explains the staggering degree of discord regarding the definition and classification of MPs and NPs (Figure 2).[29] Nonetheless, there seems to be a relatively even split in the current literature between studies citing 100 nm as the upper size limit for NPs and those citing 1000 nm. Regarding a lower size limit for NPs, some studies cite 1 nm and in others the lower limit is indeterminate.[29] Particles smaller than 1 nm (10 ångströms) may be described molecularly and therefore novel nomenclature is unnecessary.

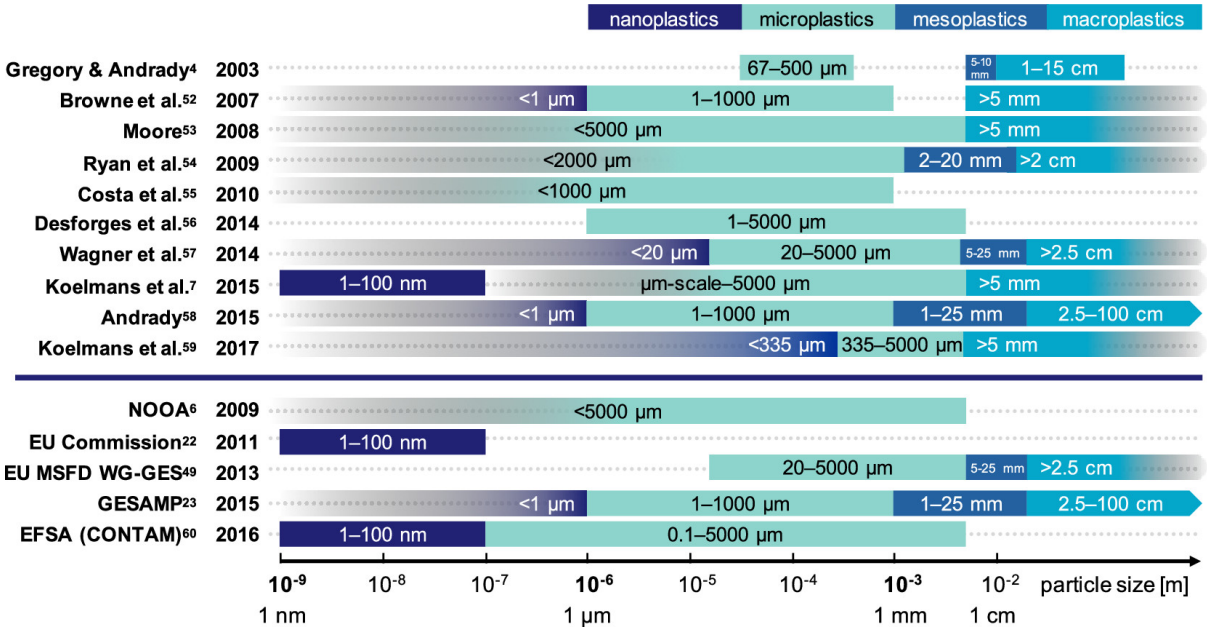

Figure 2. Plastic size classification systems.[29]

MPs and NPs may be further classified as primary or secondary.[33] Primary MPs and NPs are plastic particles that are specifically manufactured at the microscale to be used in consumer products. MPs were commonly used as exfoliants and abrasives in many personal care products such as facial scrubs, shampoo, and toothpaste prior to being made illegal in the United States in 2018 by the Microbead-Free Waters Act.[32] Preproduction plastic resin pellets (commonly referred to as nurdles) are also classified as primary MPs.[34] Primary MPs have additionally been used as sandblasting media.[14] Though smaller, primary NPs have also been used in cosmetic products as well as in research settings and some diagnostic medical procedures. Overall, any manufactured particle that enters the environment as an MP or an NP is considered primary.

Secondary MPs are those plastic particles that are produced via *in situ* fragmentation of larger plastic items within the environment.[15] The weathering of plastic waste in natural environments contributes the majority of MPs to natural systems, as fragmented plastics typically account for the majority of MPs in field surveys.[15] In fact, the fragmentation of larger plastic waste to produce MPs could account for a significant portion of the currently-unaccounted-for fraction of plastic waste in aquatic systems. Therefore, continued research looking at the fragmentation of MP and the behavior of the resulting fragments is necessary to ascertain the fate of all plastics that enter aquatic environments.

The morphologies of MPs found in aquatic systems are frequently categorized as spheres, beads, pellets, foams, fibers, films, and fragments.[29] It should be mentioned that the language used to describe these particles is not consistent throughout the literature and different authors may use different language to refer to the same morphology. For example, spheres, beads, and pellets may all refer to the same morphology across different studies. Nonetheless, in studies where the distinction is made, beads and pellets may signify that the particle is a primary MP. Beads may refer to microbeads from cosmetic products and pellets may refer to prefabrication plastic nurdles.[29] MP foam particles refer to expanded polymers with low densities such as expanded polystyrene (EPS). Foams can be open-cell or closed-cell, an important distinction that controls buoyancy and has implications for particle surface area. MP fibers are particles with one greater dimension and two shorter, relatively equal dimensions. MP films are particles with one dimension significantly smaller than the other two and may originate from the fragmentation of macroplastic films. The definition of an MP fragment is perhaps the least specific and can refer to both particles with irregular shapes as well as particles that do not fit well into any of the other morphological categories specified in a particular study.[29,33]

The morphology of NPs found in aquatic systems is much more difficult to assess given that the diffraction of visible light limits the accurate use of optical microscopy to the evaluation of particles larger than approximately 200 nm.[35] Below this threshold, techniques such as scanning electron microscopy (SEM), transmission electron microscopy (TEM), multi angle light scattering (MALS), and dynamic light scattering

(DLS) must be used.[32,36] Nonetheless, SEM requires laborious sample preparation making it an unrealistic technique when hundreds or even thousands of NP morphologies must be determined.[35] Given the difficulty of assaying NP morphology in comparison to MP morphology, less is currently known about the morphologies of NP particles collected from natural systems. An interesting deduction is that because the production of secondary NPs requires many more fragmentations than the production of secondary MPs, the morphological diversity of NPs may be less than that of MPs.[32] Indeed, one study found that the mechanical breakdown of polystyrene led to only two distinct NP morphologies, "spherical particles" and "more elongated particles."[36] Regarding primary NPs, the variety of morphologies may be comparatively more diverse given that different shapes are manufactured for specific purposes.[31] Primary NP morphologies may include spheres, used as exfoliants in personal care products, and fibers, used in textiles.[37]

1.4 Behavior in the Environment

The fate of small plastic particles in aquatic systems is governed by various abiotic and biotic processes. Chemical and physical changes that occur during these processes ultimately lead to MP fragmentation. Abiotic pathways, such as photodegradation and mechanical shearing, are commonly responsible for fragmentation of bulk plastic. The main result of plastic weathering is a decrease in average plastic particle size and an increase in plastic particle abundance.[15] Compared to macroplastic waste, MPs and NPs are likely to exhibit different behaviors and properties. Notable properties that may be altered through weathering include particle morphology, surface area, surface chemistry, density, composition, sorptivity, and toxicity.

As MP particles undergo weathering and fragmentation, total surface area increases.[33] MP surface area can control rates of biofouling (contamination with microorganisms, plants, and algae) which in turn influences effective density and sedimentation rates (Figure 3).[16,33] Increased surface area may also increase the rate that additives desorb from the particle or the rate that pollutants sorb to the particle.[38] Due to the leaching and sorption of additives and hydrophobic molecules in the environment, the chemical composition of a MP particle may differ significantly from that of the parent

macroplastic. Chemical composition can also be changed via chain scission reactions that can decrease the polydispersity index of sufficiently UV-irradiated MP particles and can lead to altered physical properties.[39]

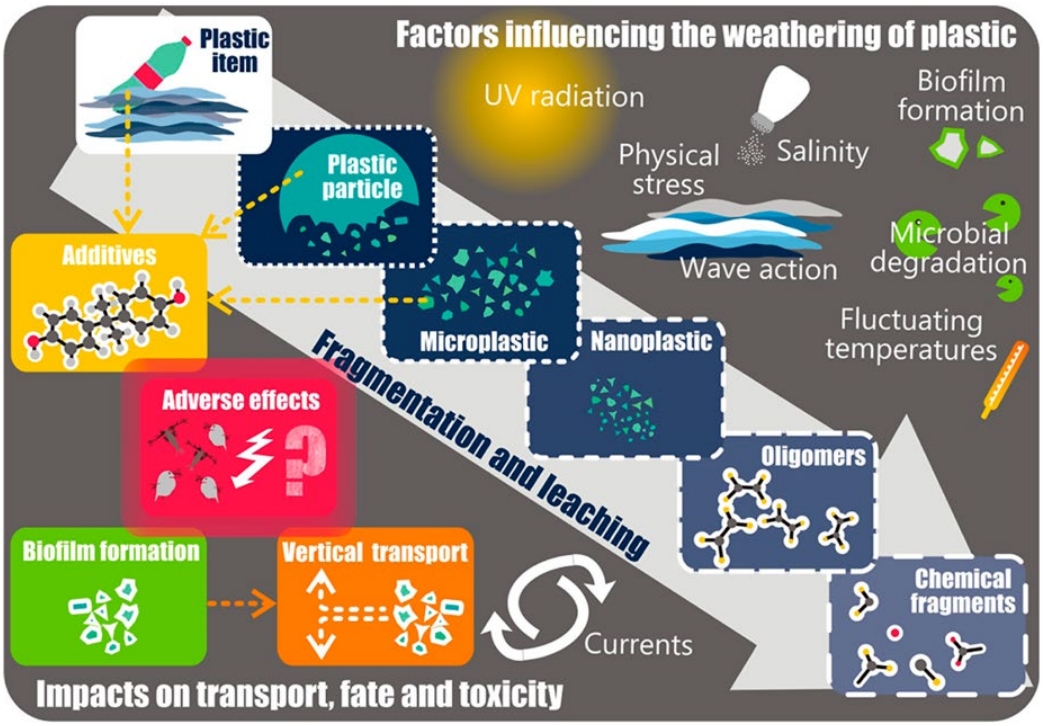

Figure 3. Plastic waste in the environment.[16]

Although NPs are produced by the same weathering processes as MPs, the scale of NPs is such that they exhibit properties distinct from those of MPs and behave differently in natural systems. Similar to MP particles, but to a much greater degree, NP particles demonstrate extremely high surface-area-to-volume ratios.[40] When a macroplastic item weathers and breaks down into NP particles in the environment, the surface area of the plastic can increase by five or six orders of magnitude. Thus, when normalized to volume, NPs may be much more potent vectors for hydrophobic molecules than macroplastics or even MPs. NP particles may adsorb more and/or faster than a similar volume of macroplastic particles.[41] Conversely, NP particles may leach additives and other sorbed molecules much faster than a similar volume of macroplastics, depending on environmental conditions.

Another characteristic that distinguishes NPs from MPs is their motion in natural systems. Plastic particles at the nanoscale may be subject to Brownian motion and therefore may remain in the water column long after their MP counterparts have precipitated out and accumulated in sediments.[42] Thus, NP particles and MP particles of equal density and chemical composition may exhibit very different patterns of cycling in aquatic systems. Where MPs may eventually settle and accumulate in sediments due to biofouling or weathering, NPs may accumulate in the water column as Brownian motion prevents them from settling. Consequently, such differences in MP and NP cycling behavior could ultimately lead to very different fates within aquatic ecosystems.

1.5 Toxicity

As the presence of MPs is increasingly confirmed in aquatic systems across the globe, an important area of research has looked at the toxicity of MPs and NPs. Independent variables in toxicological investigations commonly include particle concentration, particle morphology, polymer type, particle condition, particle size, and exposure time of the organism to the plastic particles.[43] Particle size in particular has been demonstrated to be an important determinant for plastic particle toxicity. As plastic particles decrease in size from MPs to NPs, toxicity has been shown to increase.[43] This increased toxicity is due to the fact that NPs and small MPs more readily approximate the behavior of macromolecules and therefore are well-suited to infiltrate and accumulate in the organs of various biota.[42,43,44]

Much work has already been conducted looking at the effects of MPs on fish, mollusks, crustaceans, phytoplankton, gastropoda, and even coral.[43,45,46,47] In a meta-analysis of 29 studies exposing fish to plastic particles, 26 of those studies reported one or more negative impacts on the experimental fish as a result of microplastic exposure.[43] These negative health impacts include: effects on heart and lipid tissues,[48] decreased energy storage of glycogen,[49] decreased survival,[50] aberration of liver energy metabolism,[51] increased feeding time,[52] effects on body length,[53] intestinal bacterial composition,[54] and texture of muscle.[52] These data show that fish exposed to plastic particles are not as healthy as unexposed fish.

Human exposure to MPs has also been investigated for toxic effects. Currently, the most significant human exposure to microplastics occurs via ingestion and inhalation.[55] It has been estimated that humans ingest ~11,000 MP particles per year.[56] Of the MPs that are ingested, much is thought to be due to the contamination of food, particularly seafood, during preparation, processing, and transportation.[56] Some estimates for human MP intake are as high as 121,000 particles per year when inhalation of ambient air is taken into account.[57] Ambient air in indoor environments can become contaminated with microplastics through the breakdown of synthetic fabrics and textiles. Clearly then, most humans are currently ingesting large numbers of MPs, the health implications of which are currently almost entirely unknown. The risk of exposure of the human GI tract to plastic particles should be determined given the high number of MP particles that humans ingest every year. *In vivo* MP exposure studies involving non-human mammals are scarce, yet may be key to determining the toxicological hazards posed by MPs to human health.[56]

While exposure of *in vitro* human cells to MPs and NPs has indeed shown reduced cell viability, the degree to which those results imply a hazard to overall human health remains to be determined.[57,58] Even though no controlled *in vivo* studies of plastic particles in the human body have yet been conducted, there is evidence of plastic particle toxicity based on health data from incidental inhalation in industrial settings and also from patients injected with NPs used as drug delivery vectors in various therapeutic procedures.[43] Similarly, accumulation of plastic particles in lymph nodes has been demonstrated in people with plastic prostheses.[43] In order to fully understand the threat that plastic particles pose to human health, particularly NPs within the human GI tract, much more research is needed and indeed, plastic particle toxicity is currently an emerging field in toxicology.

The ability of plastics to leach plasticizers, antioxidants, and other additives (such as BPA) represents another possible mode of microplastic toxicity to humans and other biota. Microplastics can also sorb organic carcinogens in the environment such as polychlorinated biphenyls, polycyclic aromatic hydrocarbons, and organochlorine pesticides, among others.[59,38,60] These chemicals, along with additives, can desorb from plastic particles once ingested and in this way MPs and NPs may act as vectors for

carcinogens and other hazardous compounds to enter the human body. Overall, microplastics may yet prove to be benign, yet until the mechanisms of interaction with all bodily systems are known, it is irresponsible and improper to assume so.

To better understand the toxicity and behavior of environmental MPs, it is necessary to sample them directly from the environment. Although laboratory studies using standard MPs can be beneficial in some realms of MP research, if the goal of the research is to understand the behavior and toxicity of MPs in the environment, there is no substitute for MP particles that have been weathered in the environment. This is because there are myriad factors that influence the chemistry of MPs in the environment, each to a specific degree, making the accurate replication of MP weathering a very difficult proposition. Consequently, for most MP research, it is necessary to collect MP samples from the environment so that they can be counted and characterized. Because MP particles can be collected from a variety of media, there are several established sampling techniques that are available to researchers.

1.6 Sampling Techniques

MP sampling techniques can be grouped into three categories: selective sampling, bulk sampling, and volume-reduced sampling.[61] Selective sampling is the visual identification of microplastic particles in the environment and the subsequent removal of that particle from the environment and concomitant separation of that particle from its surrounding media. An example of selective sampling would be the collection and removal of anthropogenic shoreline debris for later characterization and analysis in the lab. One study that has used this approach looked at the accumulation of plastic debris along the shorelines of the North American Great Lakes.[34] Figure 4 illustrates the complexity of sorting through organic rich shorelines to select organic debris by visual examination.[34] Bulk sampling is the collection of a quantity of media from the environment (i.e. sediment, water, air, organisms) in which microplastics are suspected to exist. This method is performed without any selectivity or separation techniques in the field. An example of bulk sampling would be the collection of one cubic meter of water into a large tank for subsequent analysis in the lab. Volume-reduced sampling is the *in*

situ separation and collection of microplastics from bulk media in the environment, effectively reducing the volume of the sample that is analyzed in subsequent steps. An example of volume-reduced sampling would be the use of a manta net to filter surface water such that only particles greater than the net size are collected for further analysis. Manta nets and neuston nets have been used extensively and successfully, making volume-reduced sampling a standard technique in MP research.[8,14]

Figure 4. Plastic debris (arrows) on organic-rich shoreline.[34]

The specific technique that is chosen for a study has depended on several factors including cost, feasibility, availability, accuracy, precision, and the media from which the microplastics are to be extracted.[62] Regarding the sampling of microplastics from water, bulk sampling and selective sampling are less common. Bulk sampling of water may be inefficient for some applications due to the large volume of water that has to be collected and transported to avoid statistical counting uncertainties.[63] Such large volumes of water can be impractical to collect, store, and transport for subsequent analysis. Selective sampling can also be problematic for several reasons. A methodology for selective sampling may be carried out differently by different researchers and therefore standardization of such an approach is difficult. Additionally, microplastic particles of a certain size, shape, or color may be more difficult to spot in a specific aquatic setting and

therefore these particles may be undercounted. Good sampling techniques should minimize problems such as reproducibility, idiosyncratic researcher behavior, and undercounting.

Of these techniques, volume-reduced sampling is most widely used for the collection of microplastics from aquatic media. Commonly employed volume-reduced sampling methods include manta net trawls and neuston net trawls for surface water sampling, and bongo nets, plankton nets, continuous plankton recorders, and near-bottom trawls for water column sampling.[64] Water intake pumps have also been used for water column sampling.[63,65] Each of these volume-reduced sampling techniques allows for the filtering of large volumes of water while indiscriminately collecting possible MP particles from the water column, effectively avoiding the biases inherent to selective sampling.

1.7 Processing Techniques

Because volume-reduced sampling techniques indiscriminately collect particles during filtration in the field, such samples can contain both organic and inorganic matter that is not plastic. Contaminating organic matter can be zooplankton, phytoplankton, organisms, or biofilms.[64] Contaminating inorganic matter can be sand particles, calcium carbonate, or sediment. To remove this unwanted material from the sample, two techniques are commonly utilized. An organic matter digestion step is typically utilized to remove organic matter from the sample that is then followed by a density separation step to remove any inorganic matter from the sample.[1]

Organic matter digestions selectively break down organic material in the sample leaving the MP particles largely unaffected. There are myriad reactions that have been successfully employed to digest organic matter including the use of Fenton's reagent, a mixture of 30% hydrogen peroxide (H_2O_2) with sulfuric acid (H_2SO_4) and ferrous iron (Fe (II)).[64] This reaction proceeds by creating hydroxyl radicals and hydroperoxyl radicals which can abstract hydrogen atoms from organic matter or add to unsaturated organic compounds. These two mechanisms both create alkyl radicals that can react with O_2 to oxidize the organic matter completely to carbon dioxide (CO_2) and water (H_2O).[66]

Advantages of using Fenton's reagent include the speed of organic matter oxidation as well as the fact that it has been found to have minimal to no effect on microplastic chemistry or particle size.[67] A similar approach has successfully used heated 30% hydrogen peroxide by itself to remove unwanted organic material.[68] Another approach to organic matter digestion, specifically biological tissue digestion, employs an acid digestion using either nitric acid (HNO_3), perchloric acid (H_2SO_4), or hydrochloric acid (HCl).[64] Alternatively, potassium hydroxide (KOH), a strong base, can be used to isolate MPs from the gastrointestinal tracts of fish.[69]

In all digestion reactions, the objective is to remove unwanted organic material while leaving MP particles physical and chemically unchanged. Whether or not MP particles are affected during the digestion depends on plastic type, size, morphology, and specific reaction conditions. For example, in a 2020 study comparing organic matter digestion methodologies in the literature, the authors found that PLA and PET polymers were completely destroyed by KOH treatment.[70] The same study found that digestion using Fenton's reagent caused no significant changes to a suite of standard MP particles (polyamide, polypropylene, polyethylene, polyvinylchloride, polystyrene, and polyester terephthalate) and only caused a slight increase in the weight of PLA particles which was due to particle agglomeration.

In cases where it is of utmost importance to avoid any changes to the MP particles, enzymatic digestions can be used to clean samples of organic material.[71,64] This approach, using a series of proteases, cellulases, and chitinases, has been shown to be effective in removing up to 98% of organic matter from samples. An acknowledged tradeoff of enzymatic digestions is incomplete organic matter digestion as well as long reaction times, frequently exceeding 24 hours in duration.

After removal of unwanted organic material via digestion, MP processing workflows typically call for a density separation step wherein heavy inorganic material is separated from the less dense MP particles. This step is particularly important when processing sediment samples or water samples with high levels of suspended solids. Density separations can be carried out in aqueous solutions or in increased-density salt solutions. In both cases, the density of the separation solution is leveraged to separate denser inorganic materials that sink, from the lighter microplastic particles that float.

Because many common plastics are denser than water (e.g., PS, PVC, PET, Nylon), it is advisable to use a salt solution that is denser than water to ensure the retainment of denser MP particles as well.

The most common salt solution for MP density separations is a saturated NaCl solution (~1.2 g/cm^3) as it is inexpensive, readily available, and environmentally non-toxic.[64] Despite these benefits, NaCl density separations will not facilitate the recovery of denser microplastics such as PVC (~1.3 g/cm^3) or PET (~1.4 g/cm^3) and therefore may lead to the underestimation of MP particles. Nonetheless, recoveries using NaCl solutions can be improved by performing repeat NaCl separations.[72] Heavier salt solutions such as NaI, $ZnCl_2$, and sodium polytungstate have been successfully utilized in order to account for and recover the full spectrum of MP densities.[68,73] However, the heavier salt solutions can be more expensive and in the case of $ZnCl_2$, can exhibit greater toxicity.[64]

In MP processing protocols, density separation is followed by vacuum filtration of the supernatant to remove MPs from the salt solution for subsequent analysis. For MP recovery, submicron filter pore sizes such as 0.2 μm or 0.3 μm are commonly used.[68,74] If MPs are to be analyzed on the filter using a spectrometric technique such as FTIR, then an IR transparent filter material such as aluminum oxide or silicon, should be chosen.[74,75] If the MP particles will be removed from the filter for further analysis (for example, via pyrolysis GC/MS) or if they will be analyzed using visual microscopy, then a less specialized filter material can be selected such as glass fiber, quartz, nitrocellulose, mixed cellulose ester, or polycarbonate membrane.[68,75]

1.8 Characterization Techniques

By far the most widely employed methodology for identifying MPs in natural samples is visual examination via optical microscopy. It has been estimated that visual identification of MPs is used in 79% of MP studies.[73] Visual examination methods are frequently used on samples that are collected from surface waters in manta nets.[22] Visual microscopy is widely used because most labs have easy access to optical microscopes, the process is cheap, and visual examination is nondestructive so it can be used prior to other, more advanced characterization and analytical methodologies.[73] Visual

identification procedures for MP particles typically call for the consistent application of a series of tests to every suspected MP particle on a filter.[76] These tests generally adhere to a flow chart which will lead the researcher to classify the particle in question as either plastic or non-plastic. Because some of the tests require physical manipulation of the particle, for example to test its malleability, the visual examination approach is best suited for the analysis of MPs >200 μm as these can be readily manipulated with forceps and identified within the magnification ranges of typical optical microscopes. However, some research groups have suggested that only particles larger than 1 mm should be analyzed via visual microscopy as accurate results for some tests can only be reliably achieved with larger particles.[22,75] Characteristics that are frequently used to differentiate MP particles from other particles include particle color, particle shape, particle transparency, presence/absence of cell-like structures, response to physical stress, and response to heat, among others.[76] The smaller the particle, the more difficult these tests are to perform and the less definitive the results.

Another technique like optical microscopy is fluorescence microscopy. With this technique, during sample processing and prior to microscopy, MPs are treated with a lipophilic dye, such as Nile Red, which will selectively stain MP particles in the absence of other organic contaminants in the sample.[77] The sample is then filtered and analyzed under a fluorescence microscope where the stained MP particles will be detectable by their fluorescence (Figure 5).[77,78] Fluorescence microscopy may enable the detection of smaller MPs when compared with optical microscopy due to the fact that even very small, clear, or otherwise difficult to detect MP particles will be stained and fluoresce. However, there are challenges in determining appropriate solvents and staining protocols for these lipophilic dyes as they will often exhibit the undesirable behavior of precipitating in aqueous solutions, making it difficult to satisfactorily stain the desired MP particles.

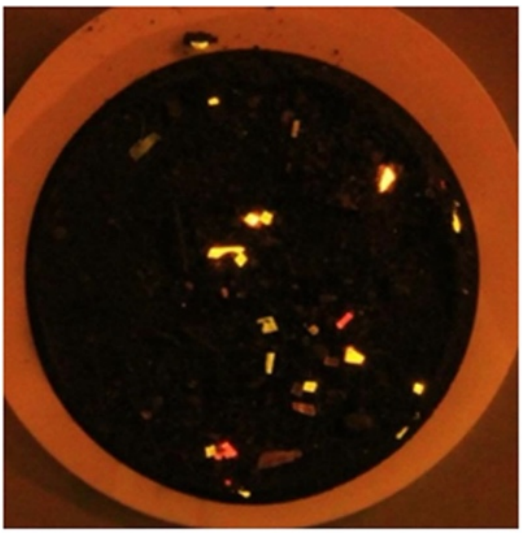

Figure 5. Control polymers stained with Nile Red.[77]

Challenges associated with the optical identification of MP particles include the fact that smaller particles are difficult to identify and subject to testing. Additionally, despite rigorous procedure instructions, particle testing may be carried out slightly differently amongst different individual researchers and this may result in discrepant conclusions regarding the same sample. If procedures are not agreed upon and assiduously followed, one researcher's polypropylene fragment could be another researcher's mollusk shell fragment. In order to reduce the possible ambiguity in particle characterization, many agree that visual identification should not be used as a standalone technique, but rather in conjunction with other more advanced methods that incorporate chemical characterization.[73]

One such advanced characterization technique is scanning electron microscopy. SEM is advantageous in that it yields excellent resolution, down to approximately 10 nm, and provides three-dimensional imagery. Because of this very fine spatial resolution, SEM can be used to visually inspect suspected MP particles to determine whether or not they are indeed plastic.[61] An additional benefit of SEM is the ability to assay the degradation of MP particles by visually inspecting the surface of the polymer for fissures, cracking, and pitting.[64] Similarly, due to the high resolution provided, SEM is an excellent approach to determine particle morphology.[75] Since SEM only yields a microscopic image, it must be paired with energy dispersive x-ray spectroscopy (EDS) in

order to determine the chemical composition of the particle in question, by way of determining its elemental composition (Figure 6).[79] This approach can provide researchers an additional datum which can be used to classify the particle as either plastic or non-plastic.[61] Because EDS provides elemental composition information, it can give useful information such as what stabilizers, antioxidants, additives, and dyes have been used to manufacture the particle in question.[64] However, it is important that suspected MP particles be thoroughly oxidized so that elemental compositions obtained by EDS do not include any sorbed biotic material.[61]

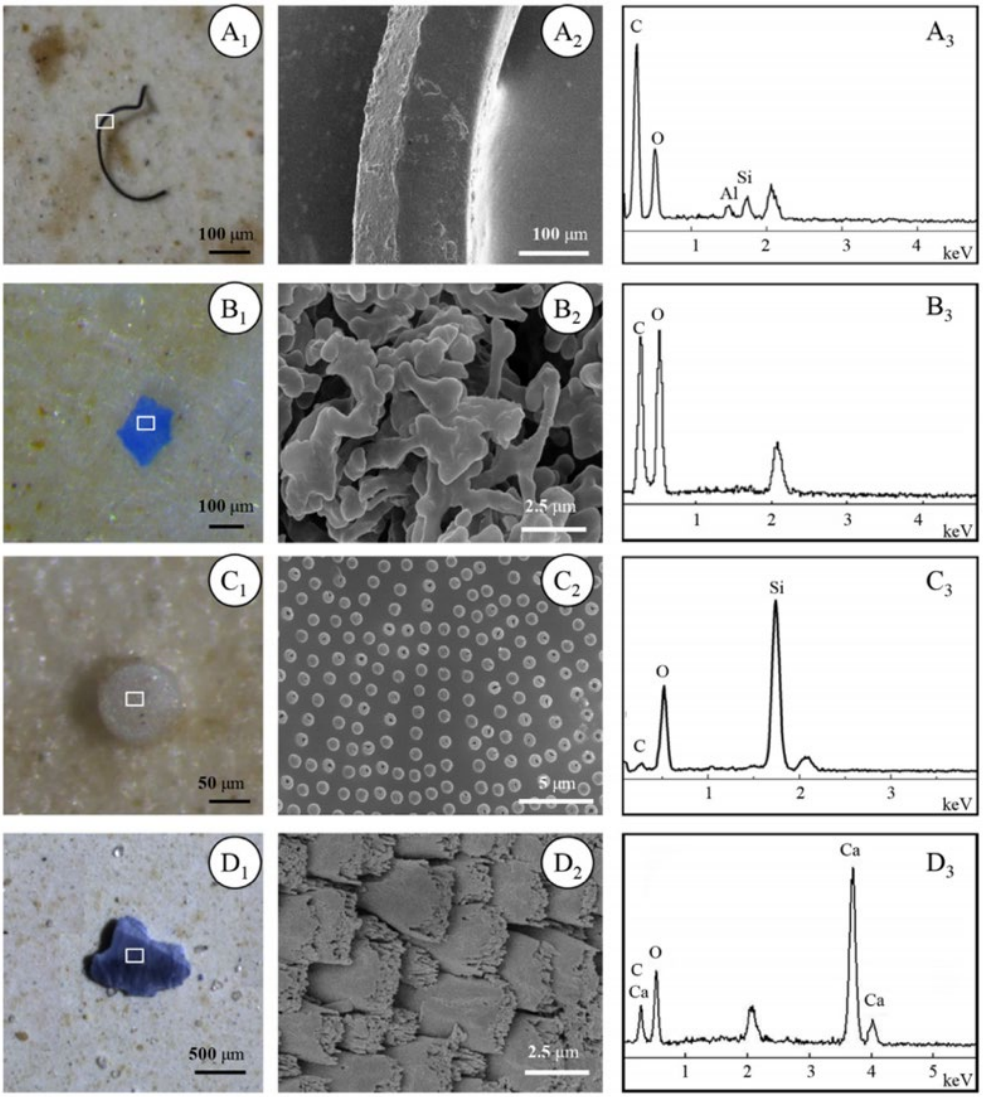

Figure 6. Optical microscope image (column 1), SEM image (column 2), and EDS spectra (column 3). Plastic particles (rows A and B) and non-plastic particles (rows C and D), diatoms and calcium carbonate, respectively.[79]

The primary disadvantage associated with SEM imaging of suspected MP particles is the significant effort that is required for sample preparation.[61,73] The extensive sample prep associated with SEM precludes the possibility of large throughput experiments or the possibility of analyzing anything other than a small portion of particles from a sample. Additionally, as mentioned above, as a standalone technique without EDS, SEM is similar to visual identification of particles, albeit at a much greater resolution. SEM alone does not give chemical composition information so researchers must be well-trained and able to differentiate plastic particles from non-plastic particles based on SEM imagery if this approach is chosen.

Another widely cited characterization technique in the MP literature is pyrolysis-gas chromatography-mass spectrometry or py-GC/MS.[75] This technique relies on the thermal decomposition (pyrolysis) of a small quantity of the sample. Typically only 50-500 µg is required.[64,80] The volatilized sample is then carried by an inert gas through a chromatography column which separates the gases based on a combination of the molecules' polarity, solubility, and vapor pressure. As the gaseous products elute separately from the column, they pass into a mass spectrometer in which the sample is ionized and accelerated through an electromagnetic field which separates the ionic fragments based on their mass-to-charge ratios to yield a mass spectrum. The resultant mass spectra can then be interpreted to determine the chemistry of the sample as well as the chemistry of any organic plastic additives.[81] As py-GC/MS is a destructive technique, suspected MP particles should first be analyzed using optical microscopy so that properties such as size, shape, color, and malleability can be recorded.[61] Even though py-GC/MS can be used with extremely small masses of analyte, when utilized in MP research, particles that are analyzed via py-GC/MS must be large enough to be manually extracted from a filter and placed in a GC vial for analysis.[64]

One possible disadvantage of the small analyte quantities associated with py-GC/MS is that the analyzed quantity may not be representative of the larger plastic if the plastic does not exhibit homogeneity at small scales.[82] Another disadvantage associated with py-GC/MS is the amount of time required to run each sample. Typically, each individual sample requires between 30 and 100 minutes to analyze, making the analysis

of many samples prohibitively time intensive.[64] Additionally, py-GC/MS is destructive (vide supra) so it is absolutely necessary that all particle information is recorded during visual examination prior to pyrolysis. Overall, py-GC/MS is a stellar method for determining particle chemistry as it is not sensitive to particle size, shape, or thickness, as is the case with some other spectrometric methods.[64] However, it is best used in conjunction with a preceding visual examination step during which particle properties other than chemistry can be recorded.

Two other chemical characterization techniques that are widely used in MP research include Raman spectroscopy and Fourier transform infrared (FTIR) spectroscopy.[83] Because both techniques are purely spectrometric, they are nondestructive. While both techniques are similar, they are based on different physical phenomena and differ slightly in their advantages and information that they yield. FTIR spectroscopy involves interrogating the vibrational modes of sample molecules with IR radiation to determine chemical structure. On the other hand, Raman spectroscopy makes use of inelastic light-scattering events that occur upon radiation of the sample. These scattering events result in the energy of the input radiation being either shifted up or down and the magnitude of these shifts gives information about the vibrational modes of the sample.[83] Raman spectroscopy is advantageous in that it is largely immune to spectral contamination from water and can detect signals from non-polar, symmetric bonds. FTIR spectroscopy can only detect molecular vibrations that exhibit a changing dipole moment and is prone to spectral contamination from atmospheric moisture. However, because of this sensitivity, FTIR is excellent for detecting molecules with polar groups.[61]

One aspect of FTIR spectroscopy that has made it particularly valuable for MP research is the sampling mode known as attenuated total reflectance, or ATR. IR spectrometers equipped with ATR accessories allow for excellent IR spectra to be obtained easily, by non-experts, and with very little sample preparation.[64] In ATR-FTIR, MP particles are secured in place with an ATR anvil upon a material with a high refractive index, such as germanium or diamond, commonly referred to as an ATR "crystal". The sample particle is then irradiated with an IR evanescent wave through the crystal and will absorb portions of the IR spectrum that correspond to its molecular vibrations, yielding an IR spectrum.[83] With ATR analysis, one should be completely sure

that the particle undergoing analysis is a MP or otherwise organic particle and not an inorganic imposter, as sand or other hard substances can scratch and damage ATR crystals. Another tradeoff with ATR-FTIR is that only particles large enough to be physically removed from a filter and placed on the ATR crystal are amenable to analysis. Typically, this means that only particles larger than 500 μm are suitable for ATR interrogation.[64] Nonetheless, ATR-FTIR has been used to great effect as a tool to verify the chemical composition of particles that have been previously identified as likely MP particles, per optical microscopy.[13]

For the identification and characterization of particles smaller than 500 μm, microscope spectrometric techniques are necessary. Micro Raman and micro FTIR techniques are, again, similar, and both are widely prevalent in the MP literature.[73] Both μFTIR and μRaman experiments can be performed in reflectance mode or transmission mode. μFTIR experiments can additionally be performed in ATR mode using a specialized micro-ATR tip accessory. Advantages of μRaman spectroscopy over μFTIR include wider spectral coverage and better spatial resolution (down to 1 μm).[22,61,83] Nonetheless, μFTIR has good spatial resolution itself (10-20 μm), sufficient for detecting MPs in all but the smallest size ranges.[61,83] The excellent spatial resolution of both techniques is achieved by controlling the aperture of the microscope which controls the size of the radiation beam that interacts with the sample. A small aperture allows for very fine spatial resolution, making it possible to selectively assay small particles. However, with very small aperture sizes, very little energy interacts with the sample, and this results in a final spectrum with a very low signal-to-noise ratio. Ultimately, when not enough energy interacts with the sample, the signal from the sample is lost in the noise. Micro spectroscopic methods have been a particular boon to MP research due to the fact that they combine the ability to determine particle chemistry, particle size, particle shape, and particle abundance.[83] A 2018 paper reviewing 170 MP studies conducted between 2015 and 2017, found that μFTIR spectroscopy was used in 28% of the studies and μRaman in 14%.[73]

In studies utilizing μFTIR spectroscopy, the supernatant of density fractionations may be filtered directly onto IR transparent filters for analysis. The filter must be made of an IR transparent material, such as aluminum oxide or silicon, so that when spectra are

taken, there is minimal spectral interference from signals originating from the filter itself. If the filter material is not strongly absorbing in the IR spectrum, then the obtained spectra will contain signals only from the particles on the filter, as desired.

After sample particles are transferred to a filter, the filter is then placed on the stage of the microscope and the surface of the filter is brought into focus. Once the filter is in focus, there are several reported procedures in the literature that have been successfully followed to detect and acquire spectra from suspected MP particles. One method is to locate potential MP particles visually through the eyepiece of the microscope and then, when a particle is found, switch to the IR probe to acquire a spectrum of that particle.[73,84] An approach to automated particle detection relies on algorithms to identify particles based on their contrast with the background (i.e. the filter). When a particle is identified in this manner, the software will take a spectrum of the particle as well as a spectrum of the background near the particle so the sample spectrum is automatically background corrected.[74] With both approaches, detecting every particle on an entire filter is prohibitively labor- and time-intensive. This is because the smallest filters used for μRaman and μFTIR analyses are typically 25 mm in diameter and have a surface area of approximately 490 mm^2. To examine the entire filter surface thoroughly and systematically at a resolution of 20-100 μm is inefficient, even using the automated algorithmic approach. Therefore, it is common that only a small portion of a filter's surface is analyzed and the results from the analyzed area are extrapolated to the entire area of the filter.[74,85,86]

These aforementioned approaches are based on selective sampling of the filter surface, however, the most common approach with μRaman and μFTIR are non-selective chemical mapping experiments that produce hyperspectral images (also known as chemigrams or chemical maps).[83] In mapping experiments, between five and ten randomly selected fields of view are chosen from the filter surface. The results from the chosen fields of view are then extrapolated to the entire filter area. Fields of view are a small portion of the entire filter surface area, typically less than 10% when added together.[74,85,86] For each field of view, a chemical map is obtained by acquiring hundreds or thousands of spectra from the filter surface in a grid pattern. This is achieved by serially scanning the surface of the entire field of view using a uniform aperture size and

a step-size that matches the length of one side of the square aperture size. Mapping experiments can be performed with a μFTIR spectrometer that is equipped with either a motorized stage, to enable serial scanning, or a focal plane array (FPA) detector. The latter technique is much faster as hundreds of spectra may be obtained in parallel (i.e., at the same time) rather than serially (one after the other).[87]

The result of chemical mapping is a three-dimensional map with two spatial dimensions, x and y, and one spectral dimension, z.[83] Each pixel in the map represents a spectrum. Chemical maps display the absorbance intensity at a single chosen wavelength or integrated over a wavelength interval. These absorbance intensities may be displayed as false color images where red, for example, may indicate high absorbance or integration values, and blue, for example, may indicate low absorbance, as shown in Figure 7.[87] False color images are an efficient way to enumerate and visualize the distribution of potential MP particles within a field of view.

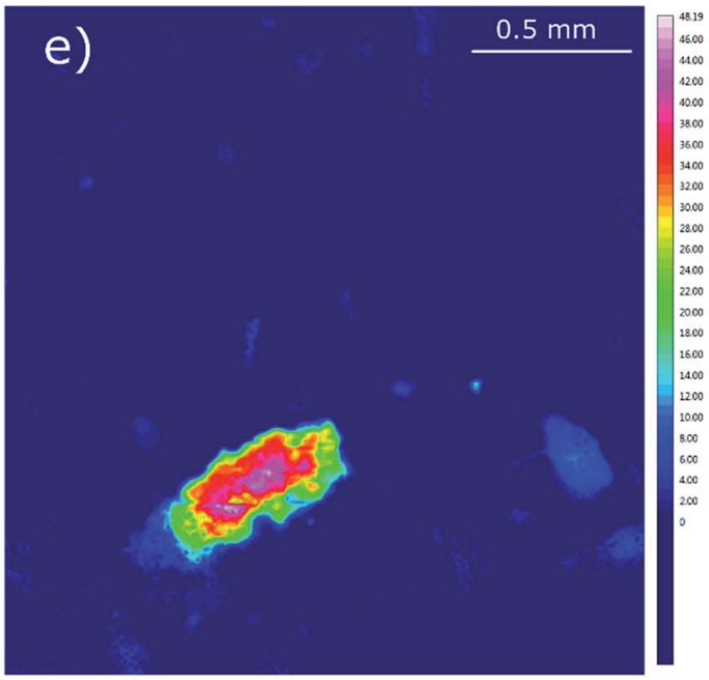

Figure 7. FPA image with absorbance from 1790-1700 cm^{-1}.[87]

After obtaining a chemical map, the data should be processed and analyzed. The data must be processed to account for the FTIR spectral acquisition mode, because spectra will differ based on their mode of acquirement.[83] This step is important, because

following processing, spectra from the chemical map are compared to spectra from reference polymer databases. These databases contain spectra that were gathered by a specific FTIR mode, such as transmission, ATR, or reflectance, and therefore the spectra that are compared to the database should be gathered by the same mode or processed to be comparable to the spectral database. By referencing a spectral database, it is possible to determine the likely chemical composition of particles contained on the filter surface.

1.9 Great Lakes Microplastics

Plastic waste enters freshwater systems in much the same way it enters the ocean system. It can either be deposited directly into freshwater systems as litter or can be entrained in wind and water and carried to freshwater systems from WWTPs, landfills, roadways, industrial districts, etc.

Regarding waste directly deposited to the environment, a 2015 review of trash collected from Great Lakes beaches noted 77-90% of all waste collected to be plastic. Of the plastic waste collected, the majority was smoking related (i.e., cigarette filters, commonly composed of cellulose acetate plastic) and items disposed of by recreational beachgoers (i.e., food containers, wrappers, bottles, etc.) with only ~1% originating from fishing related items such as buoys and fishing line. It was recognized in the review however, that these data may be biased due to the fact that the trash was collected primarily at recreational beaches and item counts were only normalized to shoreline length rather than beach area.[88] In this study, amongst all the Great Lakes, waste collected from Lake Superior beaches was notable for containing the lowest proportion of plastic waste as a percentage of total anthropogenic waste collected, at 77% compared to 85-90% for the other four Great Lakes.[88]

In addition to macroplastic litter, the transport of microplastic into Lake Superior and other freshwater lakes is an area of growing concern. While it is oftentimes impossible to determine the exact source of microplastic particles upon recovery from Great Lakes waters, several probable microplastic sources include effluent from WWTPs,[88] storm water runoff,[89] riverine discharge,[88] and atmospheric deposition.[90] Microplastics may end up in wastewater collection systems due to their presence in older

personal care products (e.g., toothpaste, exfoliants, facial rubs, shampoo, etc.).[88] Prior to being made illegal in 2018, microplastics in personal care products were used as abrasives for cleaning and exfoliating. The washing of synthetic fabrics in washing machines is also known to release large amounts (i.e. greater than 1,900 particles per cycle) of plastic microfibers into wastewater collection systems.[91] Unless WWTPs use advanced filtration techniques such as microfiltration, micro-screens, sand filtration, or mixed media filtration, MPs from these sources are unlikely to be removed from otherwise-treated waters and will be discharged in WWTP effluent.[88] Even if MPs are removed from water at WWTPs, solid residue from WWTPs is frequently used as fertilizer and compost material on agricultural fields. Thus, microplastics in these solid residues may be remobilized in agricultural runoff and ultimately transported to rivers and lakes.[88]

One study of plastic waste along the shorelines of Lake Erie and Lake St. Clair, located between Erie and Huron, looked for these smaller MP particles (<5 mm) and found preproduction plastic resin pellets to be a likely source of microplastic to Great Lakes waters, particularly among the more heavily trafficked and populated lower Great Lakes.[34] The study determined that resin pellets could end up in the lakes as a result of spillage during transport on the lakes. It was also hypothesized in this study that plastic pellets spilled in factories and along railroads could be entrained in drainage water and ultimately wend their way to the Great Lakes.[34] Although it is unlikely that nurdles from plastic manufacturers in the lower Great Lakes[92] will reach Lake Superior, due to gravitational flow from Lake Superior to Lake Huron, the Lake Superior watershed itself contains at least one plastic manufacturer, Charter NEX in Superior, WI, which uses nurdles to fabricate blown plastic film. Furthermore, given that the ports of Lake Superior handle a large volume and variety of freight, Lake Superior may be at risk for nurdle spills similar to the one that took place in 2008 when a large volume of nurdles was released to Lake Superior from a derailed hopper car near Rossport, Ontario.[93] Nurdles have in fact been identified amongst plastic waste in Lake Superior, yet only in small quantities when compared with other plastic waste morphologies.[89]

Storm water runoff from roadways and cities may also transport large quantities of MPs to aquatic systems. MPs may occur in urban areas through the natural weathering

and fracturing of larger plastic items such as vehicle parts, polymer paints and coatings, and food packaging.[14] MP abundances in the Great Lakes have been shown to be greater near urban areas and storm water runoff may be a contributing factor.[88] MP particles from sandblasting media have also been hypothesized to contribute to the MP load entering the Great Lakes via storm water runoff.[14] It should be mentioned that in contrast to the other Great Lakes, the watershed of Lake Superior is relatively undeveloped with a population density of only 5.3 people per square kilometer.[94] The two largest urban areas are the Twin Ports Metropolitan Statistical Area (Duluth, MN and Superior, WI; population 288,648) and Thunder Bay, Ontario (population 110,172). In addition to MPs in direct runoff from urban areas, rivers may carry MPs to the Great Lakes from any location within the entire drainage basin. For example, plastic particles deposited onto snow from the atmosphere may be carried in snowmelt along natural drainage systems and end up in the Great Lakes.[95]

Direct atmospheric deposition is another possible source of microplastics in the Great Lakes. In one study quantifying microplastics in Lake Superior water, a large proportion of recovered MPs were determined to be fibers[89] that are prone to atmospheric transport and deposition.[90] On the other hand, recent research has suggested that MP fiber morphologies are common products of photodegraded plastic films and sheets, implying that the fiber morphology could be produced *in situ* in aquatic systems from larger plastics of other morphologies such as films or sheets. Indeed many MPs, not just microfibers, may be formed *in situ* within the Great Lakes due to the weathering and fracturing of larger plastic items.[15]

Only a handful of previous studies have investigated the number of MPs in Lake Superior and reported particle counts, morphological data, and plastic type data. A survey of surface waters at five locations in Eastern Lake Superior in 2012 found particle counts ranged from 1,277 to 12,645 particles per square kilometer of surface water.[14] MP morphologies identified in this study included fragments, foams, pellets, films, and fishing line. A comprehensive identification of plastic type was not conducted in this study. Another study that sampled Western Lake Superior during the summers of 2016 and 2017 investigated the concentration of MPs in surface waters. The locations for this study included five near-shore locations, two open water locations and two locations in

the Duluth-Superior harbor and estuary.[89] This study was the first to present MP counts for Western Lake Superior surface waters and found areal particle counts ranging from 0 to 76,000 particles per square kilometer of Lake Superior surface water. The range of particle counts per square kilometer of surface water was 0 - 76,000 for near shore locations, 25,000 - 54,000 for open water locations, and 21,000 - 110,000 for the harbor and estuary. This study determined that the most common types of MPs in Lake Superior surface waters are PVC, PP, PE, and PET (Figure 8) and found that fibers, fragments, and films are the predominant morphology of MPs in Lake Superior surface waters.

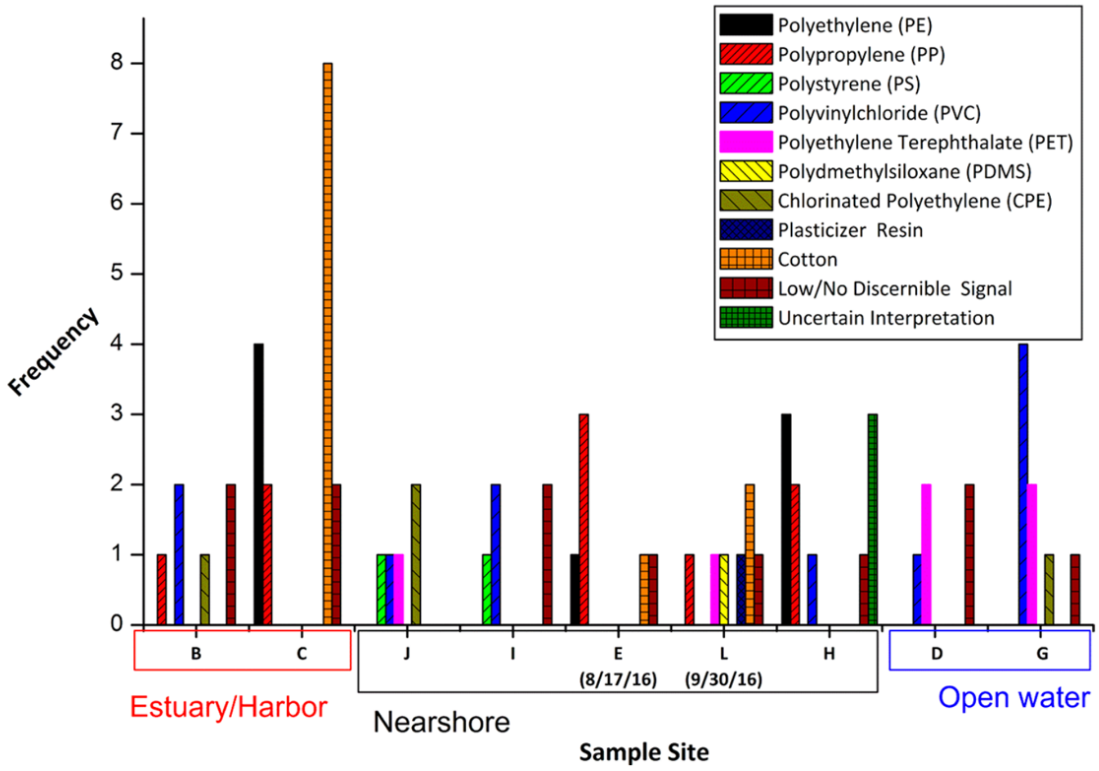

Figure 8. MP compositions in Western Lake Superior.[13]

There are several possible explanations for the abundance of fibers in Lake Superior surface waters, among them is a recent study from Maurer-Jones and coworkers.[96] This study showed that PP, PE, and PET polymer films and sheets placed in freshwater and then exposed to both artificial and solar UV-radiation led to the formation of secondary MPs via photodegradation. Of the secondary MPs that formed, fibers were the most abundant morphology observed. Furthermore, 25 µm plastic thin films that were

UV-irradiated and then subjected to turbulent water conditions produced 2.3 - 3 times as many secondary MPs as the same thin films under stagnant water conditions. Similarly, thicker 50 µm films and 3.1 mm thick sheets under the same radiation and turbulent water conditions produced 1.4 - 2 times as many secondary MPs as the same sheets under stagnant water conditions. These data would suggest that MP fibers, rather than all being transported to Lake Superior waters via effluent streams or by atmospheric deposition, can also be created *in situ* through the combined degradative processes of photooxidation and mechanical strain acting on pre-existing MPs within Lake Superior waters.

Regarding the size distribution of microplastics in the Laurentian Great Lakes, a 2013 study in Lakes Superior, Heron, and Erie determined that out of the three MP size ranges (0.355 -1 mm, 1 – 4.75 mm, and >4.75 mm) the smallest size ranges contained the greatest abundances of MP particles.[14] Specifically, the 0.355 -1 mm fraction contained 82% of all particles found, the 1 – 4.75 mm fraction contained 17%, and the >4.75 mm fraction only contained 2%. This result could be explained by the fact that as plastic items in aquatic systems are exposed to UV irradiation and mechanical abrasion, they break down into smaller particles that are themselves more numerous. This has been shown to be the case in vitro for particles between 50 and 1000 µm in controlled experiments.[15] In fact, the fragmentation of plastic particles is expected to follow an inverse third order power law.[8] The expectation is for one 1x1x1 mm plastic cube in the open ocean to break down into one thousand 100 µm fragments and eventually one million 10 µm fragments, assuming the plastic fragments in all three-dimensions. This results in the commonly observed situation where environmental plastic concentrations are inversely proportional to particle sizes.[97]

Overall the motivation for the following research stems from the fact that the vast majority of previous MP research concerning the North American Great Lakes has focused on samples collected from shorelines,[34,92] sediments,[98,99] and surface waters.[13,14,100] As of 2015, there had been no research looking at the vertical distribution of MPs throughout the water column in any of the Laurentian Great Lakes.[88] Since that time the water column has remained unsampled and uninvestigated in Great Lakes MP research, apart from a single study published in 2019.[101] In that study, one near-shore location in Lake Michigan just outside the Milwaukee break wall was sampled four times

at five depths, 0 - 13.7 meters, across a span of five months. This research was primarily an investigation of MP contamination in riverine waters in the Milwaukee River Basin, not open water locations in the Great Lakes. Sampling locations included the Kinnickinnic River, the Menomonee River, and the Milwaukee River at upriver sites and downriver sites as well as an inner harbor site, an outer harbor site, and the previously mentioned near-shore site in Lake Michigan. In this study, samples were collected with nets either towed behind a boat (for the harbor and near-shore samples) or submerged in the river at a fixed location (for the riverine samples). Notably, at the three non-river sampling sites - namely the inner harbor, outer harbor, and the near-shore site - the authors found there to be no difference between the concentration of surface water MPs and subsurface MPs. This result would suggest that MPs may be equally as prevalent in Great Lakes subsurface waters as they are in surface waters, in turn suggesting that previous studies aiming to gauge MP waste in the Great Lakes have been inaccurate due to the sampling error of excluding the water column from consideration as a potential sink for MP particles.

The rationale for sampling surface waters for microplastics is that common polymers such as polyethylene and polypropylene are less dense than freshwater and therefore, in theory, should float. However, as mentioned previously, many plastics such as PVC, PET, and PLA are denser than freshwater and should not be expected to float. Additionally, MPs floating in surface waters may undergo biofouling which can increase their density causing them to sink through the water column.[22,102] As biofouled plastics sink to depths that cannot be reached by sunlight, they may in turn become defouled as the biota they host are no longer viable in the darker, colder depths.[103] Such repeat cycles of fouling and defouling have been observed, effectively showing that MP particles should not be expected to be concentrated only in surface waters, but rather throughout the entire water column. It has also been found that small plastic particles lose buoyance much more quickly than larger plastics particles.[104] This is because small MP particles have much higher surface-area-to-volume ratios than larger plastic items, and therefore can become more biofouled (i.e., heavier) per unit of volume.

1.10 Research Motivation and Objectives

The driving hypothesis of this thesis is that MP particles are present not only in Lake Superior surface waters but throughout the water column as well. To test for the presence of MP particles in the water column, we will gather samples from surface waters and the water column. Specifically, we will sample water from the surface, the near subsurface (0.5 and 2 meters), and at depth, with some of the deeper samples well below the seasonal thermocline and others near the base of the thermocline. The thermocline coincides with the pycnocline, the depth with the greatest increase in water density per unit depth. We chose to collect samples from the chlorophyll maximum, a proxy for the pycnocline, because we expect that if microplastics are becoming neutrally buoyant in Lake Superior due to biotic processes, such as biofouling, then they should become concentrated at the pycnocline where the increase in water density will prevent previously buoyant particles from sinking further. The expected outcome of this research is a better understanding of the fate of MPs in Lake Superior and whether they are present in the water column.

To carry out water sampling, we will use a variety of novel techniques including manta net trawls, Niskin bottle volume sampling, in situ McLane pump volume-reduced sampling, and a filtration tower for near-surface volume-reduced sampling. Niskin bottles have been used in at least one previous study to sample water for microplastics in Lake Superior, Lake Michigan, and Lake Huron.[105] However, in that study, they were used to collect microfibers from surface waters, but not the water column. Similarly, in situ volume-reduced sampling has been successfully utilized in previous MP research,[63,106] but so far has not been employed in Great Lakes waters.

Another research objective is to determine the size distribution of Lake Superior MP particles between 5 μm and 333 μm, a previously uninvestigated size range. It is likely that due to degradative processes, MP particles collected from Lake Superior will be most abundant in our smallest size range (5 - 50 μm), least abundant in our largest size range (>333 μm) and will adhere to an inverse third order power law. To investigate this, we will quantify MP particles gathered from the Lake Superior water column in five different size ranges, 0.45 - 5 μm, 5 - 50 μm, 50 - 100 μm, 100 - 333 μm, and 333 - 4000

μm. The expected outcome of this investigation is a better understanding of the sizes of MPs that are most abundant in Lake Superior.

Finally, to achieve the above objectives, an important goal of this research is the development of an effective methodology for the quantification and characterization of small MP particles (<100 μm) via FTIR microscopy. Although the challenge of using μFTIR to count and characterize MPs in an effective and accurate manner has received extensive attention in the literature,[74,85,86,87,107] it is a challenge that has yet to be overcome definitively. At the moment, there is no widely implementable solution to this challenge, and approaches in the literature have either been ad hoc, proof-of-concept, or prohibitively time-intensive. Accordingly, developing a methodology for the attainment of high-quality spectra while considering time constraints and instrument limitations, promises to be a redoubtable challenge. Of note, to the best of our knowledge, this will be the first study utilizing μFTIR for MP research in the Laurentian Great Lakes.

Hypothesis

In the water column of Western Lake Superior, microplastics are abundant at the depth of the chlorophyll maximum because it coincides with the depth of the pycnocline where the increase in water density may allow trapping of microplastics that are too dense to float and not dense enough to reach benthic sediments.

Objectives

- Test novel techniques for sampling microplastics from the water column
- Examine the size distribution of microplastics in Lake Superior from 5 μm to >333 μm
- Create an automated data analysis pipeline for μFTIR spectra enabling the automatic detection of microplastic particles in natural samples

CHAPTER 2: MATERIALS AND METHODS

2.1 Overview

This research followed the steps outlined in Figure 9. Our samples were collected in Western Lake Superior during which time we filtered water with a variety of techniques and filter sizes. We then processed our samples in the lab to remove any non-plastic contaminating substances, and then analyzed via optical microscopy and FTIR microscopy. Finally, we analyzed our results to determine MP concentrations in Lake Superior

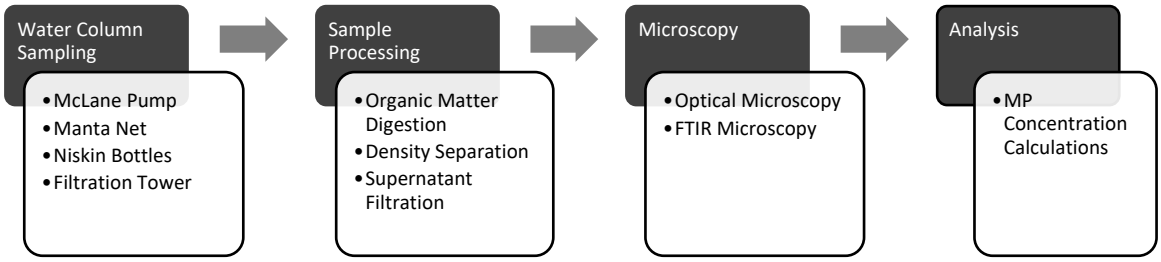

Figure 9. Research workflow and strategy.

2.2 Research Cruise

Microplastic sampling in Lake Superior took place on August 6th and 7th of 2020, aboard the University of Minnesota Duluth research vessel, the *R/V Blue Heron*. The sampling cruise was entitled Micro1. Sampling locations are outline in Figure 10. The order of station visitation was 4, 2, 7, 12. Sampling took place from 7:40am to 12:10pm on August 6th at station 4, from 3:35pm to 10:25pm on August 6th at station 2, from 12:11am to 4:45am on August 7th at station 7, and from 7:00am to 10:53am on August 7th at station 12. Sampling at the Western Mooring took place from 6:45pm on September 8th to 12:20am on September 9th and was carried out by Professor Jay Austin of the Large Lakes Observatory. These specific locations were chosen because they are sites whose water chemistry has been investigated on a seasonal basis.[108] These are also locations

where surface waters have been previously sampled for microplastic abundance.[13] Future sampling efforts at these locations, including planned sampling as a continuation of this project, will provide the temporal variability of the concentration of surface water microplastics in Lake Superior.

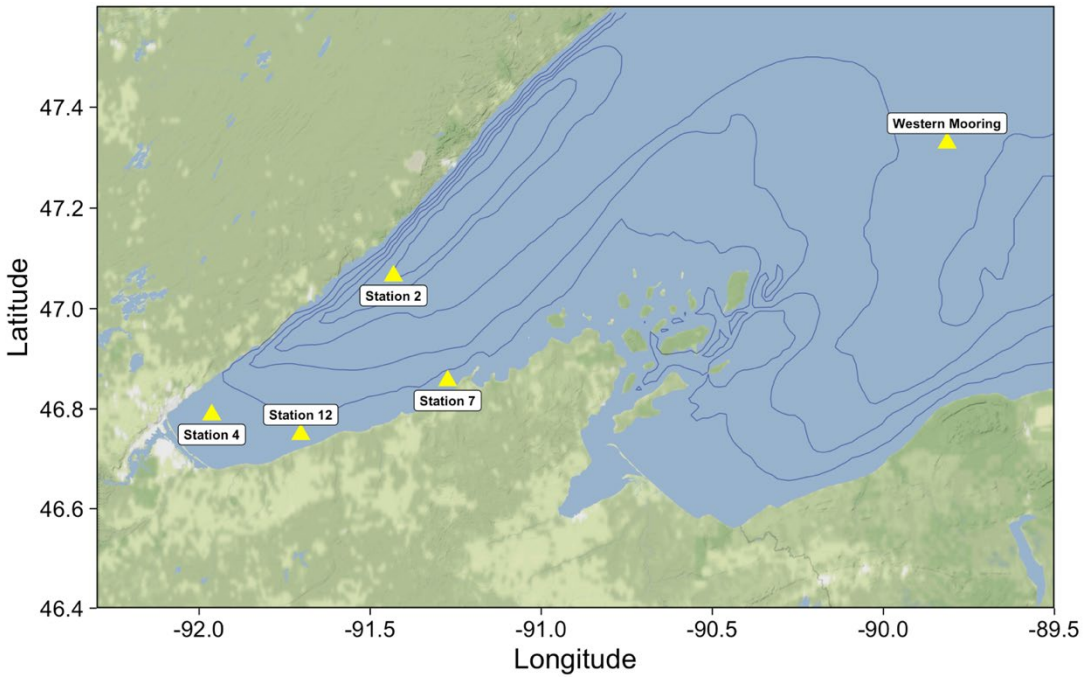

Figure 10. Micro 1 sampling locations.

2.3 Sampling

Four sampling methods were utilized to collect microplastic samples during the Micro 1 sampling cruise. These methods included (1) Manta net tows, (2) McLane pump filtration, (3) filtration tower size fractionation sampling, and (4) Niskin bottle volume sampling followed by pressurized size fractionation filtration.

2.3.1 Manta Net Sampling

Manta net tows were performed at all four locations to collect microplastics floating in surface waters. The manta net (333 µm mesh size, 3 m length, frame opening 14 cm deep by 85 cm wide, Model NQS-45-60 Series, Ocean Instruments, San Diego, CA) was attached to the end of a small marine crane with a 9.7 meter boom (Deck Crane

M95-20A3, DMW Marine Group, Chester Springs, PA) and towed off the starboard side of the vessel. Approximate one mile linear transects were completed at each station, excluding the Western Mooring. A second, shorter transect was completed at station 7 as the first tow was hindered by the build-up of organic material in the net which precluded sieving of the sample. Transect distances were calculated from the ship's GPS coordinates at the beginning and end of the transect but are complicated by the choice of projection. Transect distances were also calculated from flow meter data (Model 2030R, General Oceanics Inc., Miami, FL) (Table 1). Flow meter distances in kilometers were used for all subsequent calculations as the flow meter also accounted for any surface water movement due to wind or currents and was therefore a more accurate representation of the true volume of water sampled.

Table 1. Manta tow transect distances.

Station	GPS Distance (km)	Flow Meter Distance (km)	Surface area filtered (m^2)
4	2.124	1.79	1521.5
2	1.722	1.44	1224.0
7	0.724	0.55	467.5
12	0.644	0.50	425.0

After traversing a transect, the manta net was raised vertically from the water using the deck crane and sprayed from the outside with lake water such that all netted debris was rinsed to the cod end of the net. The cod end was then carefully removed and sieved through a 4 mm brass sieve (U.S.A. Standard Testing Sieve No. 5, Fisher Scientific Company, Pittsburgh, PA) to remove any particles larger than 4 mm, followed by a 250 µm brass sieve (U.S.A. Standard Testing Sieve No. 60, Fisher Scientific Company, Pittsburgh, PA) to collect all particles greater than 250 µm. Accordingly, the upper size limit for the manta trawl samples was 4 mm and the lower size limit was 333 µm, despite the use of a 250 µm sieve. The material collected by the 250 µm sieve was then rinsed into a glass jar with Milli-Q water for storage and subsequent processing and analysis. The manta net was rinsed with lake water before initial deployment and without the cod end to avoid cross contamination of the samples. Ambient blanks were collected

during sieving and sample handling (i.e., any time the sample was exposed to the atmosphere) to account for ambient particles that might settle onto the sieves during sieving. Ambient blanks were empty petri dishes that were opened (i.e., exposed to the atmosphere) for the duration of sample sieving.

2.3.2 McLane Pump Sampling

Sampling of the water column with the McLane pump (Water Transfer System-Large Volume Deep, McLane Research Laboratories, East Falmouth, MA) took place at a depth of 2 meters at all sampling locations, including the Western Mooring. At selected locations we also sampled the bottom of the thermocline/chlorophyll maximum region. This allowed us to test the hypothesis that if microplastics are becoming neutrally buoyant due to biotic processes, such as biofouling, then we would expect those microplastics to be concentrated where there is a significant change in water density and where there is the greatest concentration of biotic organic matter. In this work, we are interpreting the chlorophyll max as a proxy for the depth with the highest concentration of biotic organic matter. Chlorophyll max depth was determined using a chlorophyll-a fluorometer mounted to the CTD rosette (SBE 911plus CTD, Sea-Bird Scientific, Bellevue, WA). A well-defined chlorophyll maximum was present at both station 2 and station 7 and was sampled. At station 4, a well-defined chlorophyll maximum was not present, so instead a sample was collected from the benthic nepheloid layer (BNL) at 26 meters, as identified by beam extinction (C-Star Transmissometer, Sea-Bird Scientific, Bellevue, WA). Samples were collected from the hypolimnion at stations 2 and 12, from depths of 240 and 18 meters respectively. There was no near-bottom beam extinction at stations 2 and 12 so neither of these deep samples were collected from a BNL. Station 2 was the deepest station sampled with an overall water depth of 257 meters. For a summary of samples collected with the McLane pump, refer to Table 6.

Pumping and filtering was performed *in situ* to collect microplastics from the water column. Before each deployment, the McLane pump was backflushed with 5 liters of Milli-Q water to prevent air from entering the pump. After backflushing, a 142 mm diameter, 100 μm nylon mesh filter (McMaster-Carr, Elmhurst, IL) was placed in the filtration manifold of the McLane pump (Figure 11). Pump parameters were then set via a

hard connection to the McLane pump from a Windows terminal loaded with Crosscut software from McLane Research Laboratories. Sample volume was set to 200 liters, initial flow rate was set at 4 liters per minute, and the time limit was set to 65 minutes with a minimum flow rate of 2 liters per minute and an initial 15-minute countdown from the time of system deployment via Crosscut to the start of pumping. After deploying the system at the terminal, the wired connection was removed and the connection port on the pump was replaced with a watertight dummy plug. The pump was then attached to the A-frame steel cable and lowered to the appropriate depth off the stern for the duration of pumping. Upon expiration of the pumping period, the pump was raised from the water column and detached from the winch cable. The filter was immediately retrieved from the filtration manifold and placed in a jar with 100 ml of Milli-Q water to prevent drying and adhesion of microplastics and organic material to the mesh filter during storage.

Figure 11. McLane WTS-LV Deep.

2.3.3 Filtration Tower Sampling

Near surface sampling of the water column was performed utilizing a custom-built filtration tower (Figure 12) based on the design originally conceived and described by Martin et al.[109] The filtration tower contained a serial filter cascade with top-to-bottom

filter sizes of 300 µm, 100 µm, 50 µm, and 5 µm. Filters were located at the four PVC union joints for accessibility. Union joints were kept watertight with rubber O-rings. The 5 µm and 50 µm filters were ~108 mm in diameter and fixed in place by the O-rings pressing against the union joints. The 300 µm filter was 63 mm diameter and was secured in place by only the internal interface of the union joint. To secure the 100 µm nylon filter (63 mm diam.) in place, a 76 mm diameter, 864 µm wire mesh disc was placed at the union joint to support the filter so that it would not be pushed downwards by the flow of water through the cascade.

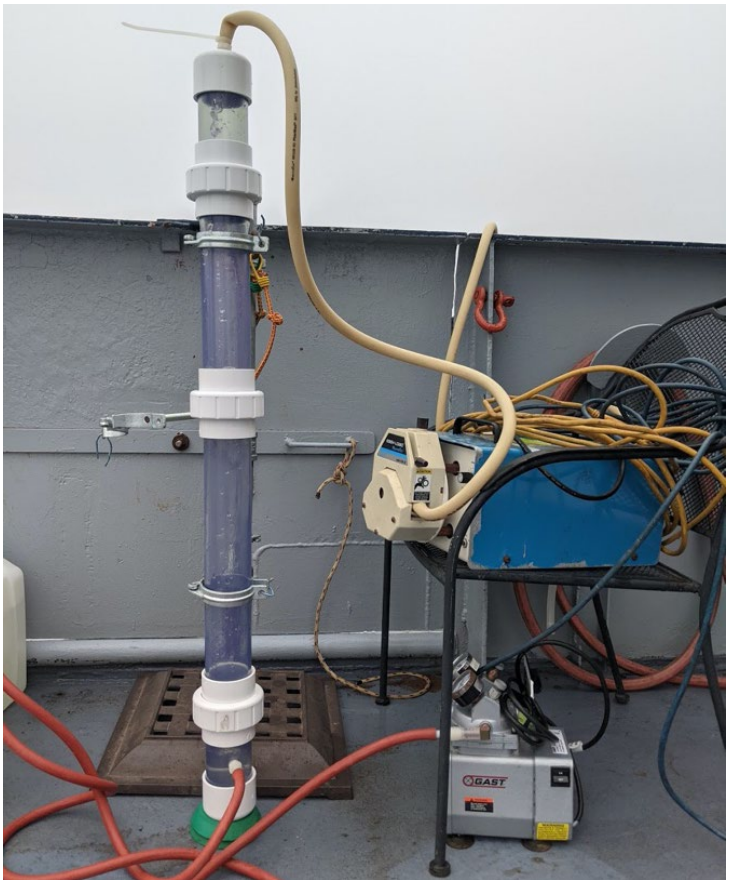

Figure 12. Filtration tower.[109]

A peristaltic pump (Cole Parmer Masterflex Peristaltic Pump with easy-load Masterflex pump head, Cole-Parmer, Vernon Hills, IL) with Masterflex tubing (Masterflex L/S Precision Pump Tubing, PharMed BPT, ½ in. ID, Cole-Parmer, Vernon Hills, IL) was used to draw water over the gunwale of the *R/V Blue Heron* to the top of

the filtration tower. Water was drawn from a depth of 0.5 meters. 100 liters of lake water was filtered through the tower at each of the four stations. After filtration, each filter was carefully removed and placed in a glass jar with 100 ml of 0.2 µm filtered ultrapure Milli-Q water to prevent drying and adhesion of microplastic and organic material to the mesh filter. Glass jars were then packed for storage and subsequent processing and analysis. The filtration tower was rinsed with Milli-Q from the sampling site before each sampling run to avoid cross contamination of samples. Ambient blanks were collected during filter placement and during filter removal to account for ambient particles that might settle onto the filters during exposure to ambient conditions. Ambient blanks were empty petri dishes that were opened for the duration of filter handling. Validation testing of the filtration tower is described in Appendix A.

2.3.4 Niskin Bottle Volume Sampling

Because the McLane pump is not a well-established technique for sampling the water column, we devised another method for water column sampling to compare the two techniques in terms of facility. The method we conceived involved volume sampling from the water column using Niskin bottles, followed by immediate filtering of that water aboard the *R/V Blue Heron*.

At each of the four sampling locations, CTD rosette mounted Niskin bottles were used to collect 20 liters of lake water from a depth of 2 meters and from the chlorophyll max. The chlorophyll max was determined using the chlorophyll-a fluorometer on the CTD rosette. At station 2, a sample was collected from the hypolimnion as well (240 meters). After the Niskin bottles were sealed at their respective sampling depths, the rosette was raised and the contents of the Niskin bottles were drained into separate stainless-steel Cornelius kegs (AEB Kegs, Vimercate, Italy) according to the depth of collection. Each keg was then sealed and pressurized with nitrogen gas. The water was then pushed from the kegs and ran through a stainless-steel filtration manifold (Figure 13with three mesh nylon filters (100 µm, 50 µm, and 5 µm), each 47 mm in diameter. After filtration of the 20 liters of water from the Niskin bottles, the filters were removed from the filtration manifold and placed in jars with 100 ml of Milli-Q water to prevent drying and subsequent adhesion of material to the mesh filter. Glass jars were then

packed for storage and subsequent processing and analysis. Additionally, the first liter of filtrate from the filtration manifold was run through a 0.45 µm mixed cellulose-ester (MCE) filter in an all-glass filter rig to capture the 0.45-5 µm size fraction of microplastics. The 0.45 µm MCE filters were also stored in 100 ml of Milli-Q water for later laboratory processing and analysis. Validation testing of Niskin bottle sampling is described in Appendix B.

Figure 13. Filter manifold with stainless-steel keg.

2.4 Processing

Following the Micro 1 cruise, all samples collected aboard the *R/V Blue Heron* were placed in jars containing 100 ml of Milli-Q water to prevent drying and adhesion of microplastics and organic material to the mesh filters. Jars were stored at the Large Lakes

Observatory in a 5°C walk-in refrigerator while they awaited processing. This prevented a malodorous scent in the lab and reduced the possibility of organic matter growth in the samples which would require more aggressive and longer oxidations.

In-lab processing of each sample began by placing the sample jar in an ultrasonic bath (Ultrasonic Cleaner, Branson Cleaning Equipment Company, Shelton, CT) for 5 minutes. This was done to loosen particles that might still be clinging to the filter or interior of the jar. After ultrasonication, the filter was raised from the jar with clean metal forceps and thoroughly rinsed with Milli-Q water. The rinsed nylon mesh filter was then removed and the jar containing the sample in Milli-Q water was placed in an oven at 90°C. Complete evaporation of water took 2-3 days resulting in a dry glass jar containing all the organic material, particulate matter, and microplastic particles that were collected during filtration.

To remove the non-plastic organic material from the sample and transform it to carbon dioxide (CO_2) and water (H_2O), an oxidation step was performed. The dry glass jar containing the sample was placed on a hotplate in the fume hood and a PTFE magnetic stir bar was added to the jar. A thermometer was inserted into the jar and 20 ml aqueous 0.05 M ferrous sulfate heptahydrate ($FeSO_4 \cdot 7H_2O$) was added and brought to ~60°C. The reaction was performed while the jar opening was lightly covered in aluminum foil to prevent any ambient particles from entering the reaction vessel. To this solution was added 20 ml 30% hydrogen peroxide (H_2O_2, Fisher, Pittsburgh, PA) to create Fenton's reagent, a strong oxidizing reagent. This reagent is responsible for oxidizing the organic material to carbon dioxide and water.[66] As the ferrous iron reacts with the hydrogen peroxide, a highly exothermic reaction, the temperature of the reaction was controlled so that it never exceeded 90°C. Modulating the temperature was achieved by removing the jar from the hotplate or by adding room temperature Milli-Q water to the reaction. Once the reaction ceased to energetically effervesce, the reaction was monitored and allowed to proceed until no more effervescing was visible. This was typically one half-hour. Robust effervescence typically lasted one minute. If organic material was still visible in the reaction jar after this period, an additional 20 ml aliquot of hydrogen peroxide was added to further oxidize the sample. For all samples besides the Manta net samples, a total of three aliquots of hydrogen peroxide were sufficient for complete

oxidation of the samples. For the Manta net samples, upwards of ten aliquots of hydrogen peroxide were required for complete oxidation of all organic material. An oxidation was determined to be complete when visible organic matter was minimized in the reaction jar and unchanged with further hydrogen peroxide additions.

After complete oxidation of all visible organic material in the jar, sodium chloride (previously combusted at 450°C for 12 hours) was added to the jar to make a saturated solution of sodium chloride with a density of 1.18 - 1.20 g/ml. The glass jar was then removed from the hotplate and the magnetic stir bar was drawn up the inside of the jar using a magnetic stir bar retriever on the outside of the jar. The stir bar was rinsed with Milli-Q water inside the jar and then removed from the jar. The solution was transferred to a 250 ml separatory funnel with a PTFE stopcock for density fractionation. The jar was thoroughly rinsed with Milli-Q water to ensure the complete transfer of the entire solution to the separatory funnel. The solution was then left to separate overnight in the separatory funnel in the fume hood.

After density separation, the bottom of the separatory funnel was inspected to identify any heavy inorganic or non-plastic particles that might have settled to the bottom of the column overnight. If present, these were carefully drained from the bottom of the funnel and stored in a labelled vial for later analysis.

The remaining solution and supernatant in the separatory funnel were then vacuum filtered for microscopic analysis. All samples 300 µm and larger were filtered onto 47 mm diameter gridded 0.45 µm mixed cellulose ester (MCE) filters (MF-Millipore Membrane Filter, 0.45 µm pore size, MilliporeSigma, Burlington, MA) for analysis via optical microscopy. All samples smaller than 300 µm were filtered onto IR transparent 0.2 µm inorganic filters (Whatman Anodisc, MilliporeSigma, Burlington, MA) for analysis via FTIR microscopy. The separatory funnel was thoroughly rinsed into the filtration apparatus with Milli-Q water. The filter holder was also rinsed with Milli-Q water. The filtration apparatus consisted of a glass 300 ml filter holder, a fritted glass support base with a silicone stopper, an aluminum spring clamp to affix the filter holder to the base, and a 1-liter glass vacuum filtration flask. After filtration was complete, the clamp and filter holder were removed, and the filters were carefully removed from the apparatus with clean metal forceps and placed in a properly labelled, previously

combusted glass petri dish for later microscopic analysis. All glassware used for sample processing was combusted at 450°C for 8 hours prior to use.

2.5 Quality Assurance

During the research cruise all personnel on the science team wore cotton clothing to eliminate the possibility of contaminating samples with synthetic fibers from polymer textiles like polyester and nylon. For the same reason, cotton lab coats were worn during processing and microscopy in the laboratory. As mentioned previously, all glassware was combusted at 450°C for 8 hours prior to use to volatilize and remove any possible contaminating MP particles. From sample collection through microscopy, all sample-containing vessels were consistently covered with aluminum foil to prevent the ingress of ambient MP particles, even during the oxidation reaction.

To control for possible ambient contamination of manta net samples during handling aboard the *R/V Blue Heron*, ambient blanks were obtained for each manta net cast. When the cod end of the manta net was removed, and before rinsing the sample through the 4 mm and 250 μm sieves, a petri dish was opened, sparged with Milli-Q, and taped in place beside the sieving station on the aft deck of the ship. The dish was sparged so that any ambient particles would stick in the petri dish just as they would stick to the wet sample if they contacted it during on-deck sieving. After on-deck sieving, the petri dish was closed. These petri dish samples were then individually oxidized and density fractionated in the laboratory following the same processing protocol as the samples themselves. The supernatant was then filtered onto MCE filters for visual microscopy analysis.

Unlike the sieving of the manta net samples, there were no on-board processing steps for the McLane pump samples so ambient blanks were not collected. Instead, a method blank was performed in the laboratory to control for any contamination that might occur while processing the McLane pump samples in the lab. 100 ml of Milli-Q water was placed in a glass jar and then completely evaporated in an oven at 90°C. The method blank sample was then oxidized, density fractionated, and filtered onto an

Anodisc filter for visual and computational analysis by μFTIR spectroscopy, as described below.

2.6 Microscopy

Manta net samples were analyzed using optical microscopy and the 100 μm McLane pump samples were put aside to be analyzed via FTIR microscopy.

2.6.1 Visual Microscopy

Analysis of the manta net samples was performed using a 3.5X-90X LED trinocular zoom stereo microscope with a 10-megapixel digital camera (Amscope, Irvine, CA). The petri dish containing the gridded MCE filter was placed on the microscope stage, the petri dish cover was removed, and the filter surface was brought into focus. Starting at the top of the gridded filter, each 3.1mm x 3.1mm grid square was visually analyzed for the presence of particles. Only particles larger than the mesh size that they were collected on were considered (i.e., larger than 333 μm for the Manta net samples).

All potential microplastics were subjected to a "hot needle test." This test involved heating the tip of a sewing needle with a lighter until the tip of the needle glowed red. The needle was then brought near to the particle in question to test whether the particle underwent any melting due to the heat of the needle. Particles that clearly melted were classified as microplastic particles. Melting was referred to as a "positive" hot needle test. Particles that either ignited, burned, or displayed no observable response to the heat were classified as non-plastic. This method for plastic identification was originally described by Hendrickson et al.[13] The hot needle test was not a reliable method for assaying particles smaller than 333 μm as the results of the test become less conclusive with smaller particle sizes. That is, for particles smaller than 333 μm it was difficult if not impossible to determine whether a particle ignited, melted, or remained unaffected. For each particle that was subjected to the hot needle test, the results of the test were recorded as well as the particle morphology, prior to the melt test. Some particles were photographed. Particles that were identified as plastic based on the hot

needle test and that were large enough to be handled with metal forceps were removed from the filter and collected in labelled GC vials for validation via ATR-FTIR.

ATR-FTIR testing of particles collected during visual microscopy was performed to validate the accuracy of the hot needle test. Particles were removed from their GC vials using metal forceps and placed on the diamond ATR crystal of the FTIR spectrometer (Nicolet iS50 FTIR, Thermo Fisher Scientific, Waltham, MA). The sample was then secured in place by turning the ATR anvil (the threaded assembly above the ATR crystal) until it clicked. The anvil ensures good contact between the sample and the ATR crystal and allows for equal pressure to be applied to every sample. Each sample was chemically interrogated with 64 scans at a resolution of 4 cm^{-1}. Backgrounds were taken after each sample to correct for atmospheric interference due to CO_2 and H_2O. Between each sample the ATR crystal was carefully cleaned with a Kim Wipe sprayed with methanol to avoid any cross-contamination of samples. Microplastic chemical identity was determined by comparing sample spectra to standard spectra from the sample Hummel Polymer Library that is preloaded in the OMNIC Series Software (Thermo Fisher Scientific, Waltham, MA).

2.6.2 FTIR Microscopy

Analysis of the 100 μm McLane pump samples was performed using a Nicolet Continuum Infrared Microscope attached to a Nicolet iS50 FTIR Spectrometer (Thermo Fisher Scientific, Waltham, MA). Spectra were gathered in reflectance mode. The IR microscope can perform chemical mapping by utilizing the motorized stage of the microscope. The motorized stage allows for the microscope to scan across the surface of the filter to produce a two-dimensional spectral map. On the spectral map, each pixel represents an IR spectrum that corresponds to a specific region on the filter itself. Chemical mapping is useful because it allows for all particles within a field of view to be chemically interrogated and their composition identified.

To test the ability of the IR microscope to detect MP particles on IR transparent filters, experiments were performed to determine optimal instrument settings. Instrument settings that needed to be determined included resolution, aperture size, spectral range, number of scans, spectral map (field of view) size, and the step size for mapping. These

optimization experiments were performed using MP standards of known composition, size, and morphology. Specifically, 117 µm diameter polystyrene spheres, 10-45 µm diameter polyethylene spheres, 250 µm diameter polyvinylchloride fragments, 300 µm diameter polyethylene terephthalate fragments, 350 µm diameter polyethylene fragments, and multi-size polypropylene fragments. These MP standards were filtered onto IR transparent Anodisc filters for µFTIR analysis. A background spectrum was taken of the Anodisc filter surface, and this background was subtracted from all sample spectra. To determine the ideal aperture size, spectra of a polyethylene MP fragment were taken with aperture sizes between 10 and 100 µm. Because larger aperture sizes lead to higher spectral quality yet lower spatial resolution, the goal was to determine the smallest aperture size that would reliably yield quality spectra. Apertures greater than 30 µm yielded good spectral quality (Figure 14), and an aperture size of 50 µm was chosen for all further experiments. Further, the 50 µm step size was determined by the 50 µm aperture size.

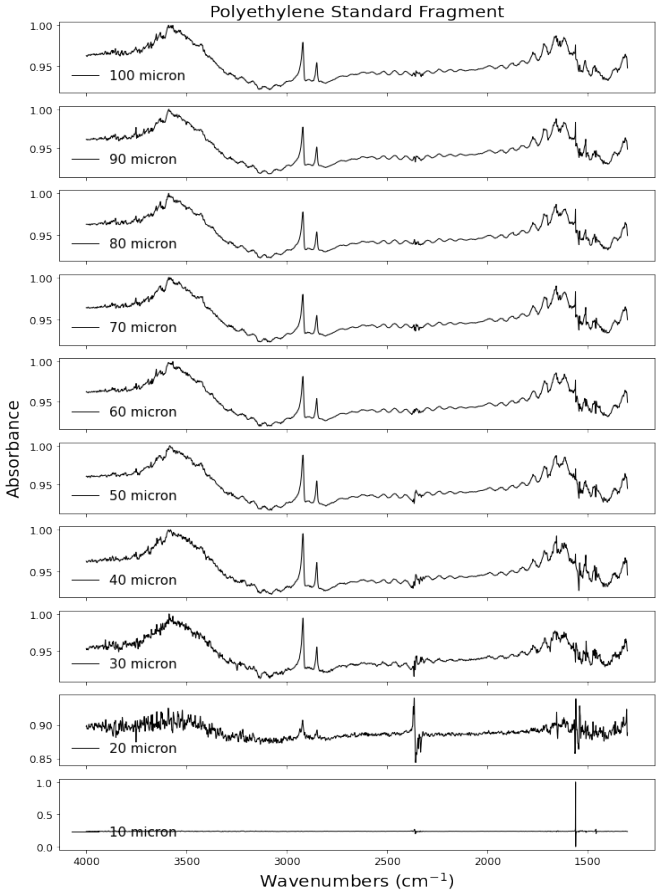

Figure 14. Aperture size experiment series (aperture size inset).

To determine the ideal number of scans, spectra of a polyethylene MP fragment were taken using 1, 2, 4, 8, 16, 32, 64, and 128 scans (Figure 15). Again, because increasing the number of scans leads to higher spectral quality yet longer experiment times, the goal was to determine the fewest number of scans that would still yield good quality spectra. 32 scans were chosen for all subsequent experiments because C-H stretching at ~2850 cm^{-1} was clearly visible above the background noise with 32 scans. A resolution of 4 cm^{-1} was chosen. Typically a resolution of 8 cm^{-1} is chosen, however with a finer resolution, peaks can be more easily distinguished from one another.[63] A spectral range of 1300-4000 cm^{-1} was chosen because below 1300 cm^{-1}, the aluminum oxide filter material is IR absorbing and interferes with the sample signal in that region. Of note, background handling is extremely difficult with reflectance IR spectroscopy, and therefore the CO_2 signal in Figure 15 is prominent around 2350 cm^{-1}.

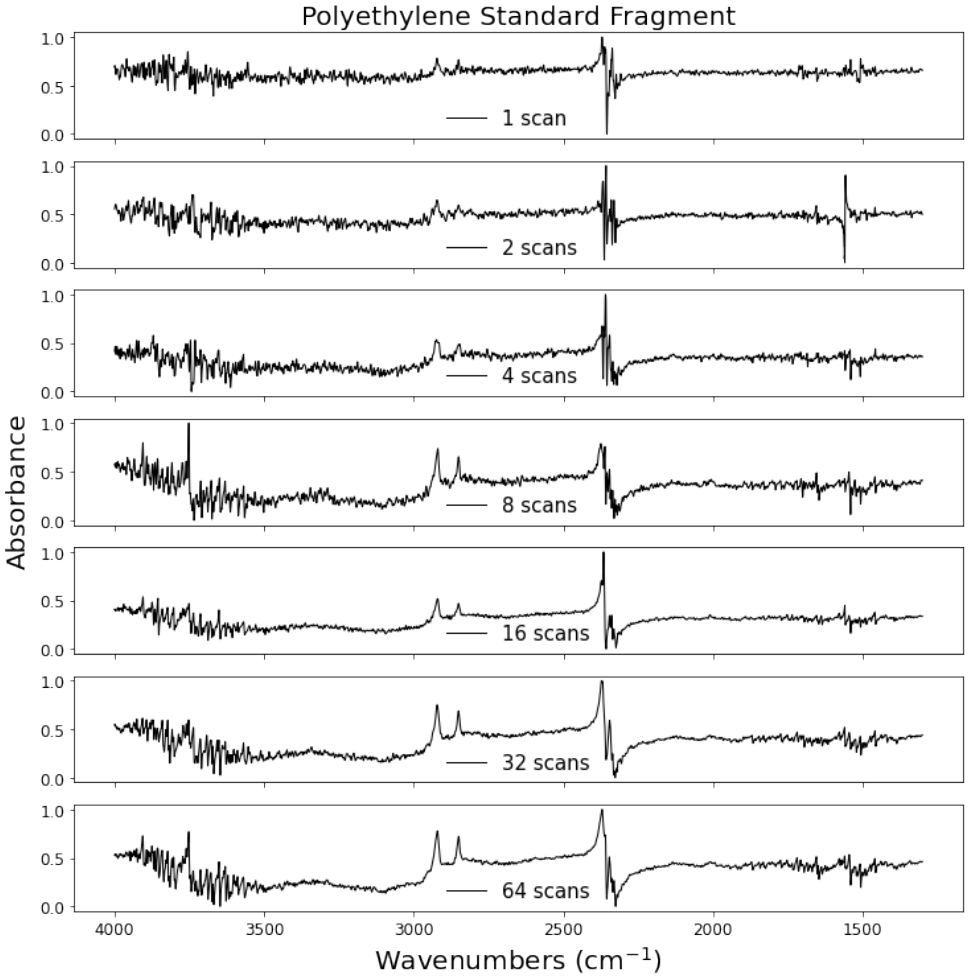

Figure 15. Scan number experiment series with PE fragment.

Finally, the size of the field of view was determined through trial and error. A larger 4x4 mm field of view was collected but this was problematic because the Anodisc filters do not sit flat on the µFTIR stage. This made it impossible to maintain satisfactory focus on the surface of the filter throughout an entire field of view, as the z-distance to the filter was constantly changing. Of note, the autofocus feature of the FTIR microscope was incapable of discerning enough contrast to function correctly to enable such experiments with 4x4 mm fields of view. Therefore, a smaller 2x2 mm field of view was chosen. Even though the 2x2 mm field of view also could not maintain perfect focus throughout the entire area, this size was chosen as a compromise between focus and efficiency. That is, if smaller fields of view were chosen, then more fields of view would have to be taken on each filter to scan the same surface area. Using a 2x2 mm field of view, all MP standard particles were identified by inspecting the chemical map at 2850 cm^{-1}. By way of the above experiments, the optimal instrument settings for microplastic identification were determined (Table 2). These settings were chosen as optimal for particle sizes 50 µm and larger.

Table 2. Continuum FTIR microscope experiment settings

Resolution	4 cm^{-1}
Step size	50 µm
Aperture	50x50 µm
Field of view	2x2 mm
Spectral range	1300-4000 cm^{-1}
Scans	32

100 µm McLane pump samples were analyzed by placing the Anodisc filters on the motorized stage of the Continuum microscope. Because scanning of the entire filter was extremely time consuming, only ten 2x2 mm fields of view were chosen for analysis. These ten fields of view were randomly chosen by the researcher. Each of the ten fields of view took seven hours to scan completely, making for a total analysis time of 70 hours per filter. Between each field of view, the microscope was adjusted to scan a new randomly chosen field of view and the focus of the microscope was refined to be sharply

focused on the center of the new field of view. Optimizing the focus at the center of the field of view ensured that the microscope never got completely out of focus, even in the corners of each field of view.

After scanning ten fields of view, the resulting chemical maps were individually analyzed to determine microplastic particle counts. Chemical maps were set to display the reflectance intensity at 2850 cm^{-1}, the IR frequency corresponding to sp^3 C-H stretching.[110] This stretching mode was chosen as the analytical frequency for chemical maps because it is present in the vast majority of plastics in production worldwide, besides, for example, PTFE which is rarely observed in natural samples. On the chemical map, pixels with low reflectance intensity (indicative of strong IR radiation absorbance) were chosen for further investigation. Because background reflectance levels are not uniform across the entire field of view, not all pixels that show low reflectance intensity at 2850 cm^{-1} are indicative of plastic particles. That is, some pixels show low reflectance intensity at 2850 cm^{-1} not because of *specific* absorbance at that frequency but rather because the entire spectrum of IR radiation is poorly reflected (strongly absorbed) at that location. This happens when there is a substance on the filter that is broadly absorbing around 2850 cm^{-1} rather than specifically absorbing at that wavelength. Such a broad absorption band indicates that the substance is not plastic. To determine whether low reflectance at 2850 cm^{-1} was due to the presence of a plastic particle, there had to be a visually distinguishable downward peak (absorbance peak) indicative of selective IR absorption due to an sp^3 C-H bond. Pixels that clearly showed IR absorbance due to sp^3 C-H bond stretching were recorded as corresponding to microplastic particles.

To aid analysis, all spectra were normalized to show absorbances between 0 and 100. Because each field of view comprised 1681 spectra, it was impractical to manually analyze each of the 1681 spectra individually. Therefore, only pixels (spectra) that displayed low reflectance intensities at 2850 cm^{-1} and corresponded to the locations of visible particles in the stitched-image photograph of the field of view were considered as potential MP particles.

Although the Anodisc filters are 25 mm in diameter, the diameter of the filtration apparatus that was used during vacuum filtration was 16 mm in diameter. Therefore, the surface area of the filter with retentate was only 201 mm^2 (16 mm diameter), as opposed

to 490 mm^2 (25 mm diameter), and the 10 x 4.2025 mm^2 fields of view that were collected constituted ~ 21% of this reduced filter surface area. Accordingly, the total MP counts from the ten fields of view were multiplied the appropriate factor of 4.78 to estimate the total number of MP particles that were present in each sample.

Importantly, because spectral quality was insufficient to determine the identity of the microplastic particles, particles were only characterized as plastic or non-plastic, as determined by the presence or absence of absorbance peaks in the sp^3 C-H bond stretching region of the IR spectrum. Accordingly, this approach answered only the most important question in MP particle analysis: Is this particle plastic or non-plastic?[74]

2.6.3 Computational Analysis

Because the process of manually searching each field of view for MPs was prone to subjective researcher error given that each field of view consisted of 1681 spectra - and to automate the entire process of MP detection - a custom Python script was written to aid in spectral analysis. This script was based on the simple idea that spectra obtained from MP particles will be strongly absorbing at 2850 cm^{-1} (the sp^3 C-H bond stretching region of the IR spectrum) when compared to the spectral baseline. In the script, a proxy for the spectral baseline was the reflectance at 2750 cm^{-1}, a region of the spectrum that is not IR absorbing for common plastics. Therefore, for each spectrum in the field of view, the difference between the reflectance intensity at 2750 cm^{-1} and 2850 cm^{-1} was recorded and only the differences that were high outliers were taken to be indicative of MP particles on the filter. Outliers were determined assuming that the histogram of differences adhered to a Gaussian distribution (Figure 16). The cutoff for determining outliers (blue line in Figure 16) was determined for each field of view using a custom-built algorithm. This algorithm iteratively sets aside high outliers until there are no more high outliers and the data adhere to a Gaussian distribution (red dashed line in Figure 16). All the spectra that were set aside during this iterative step (i.e., to the right of the blue dotted line) were considered spectra representing MP particles. This iterative approach is necessary to avoid missing particles when large amounts of MP particles are present on the filter, resulting in a bimodal distribution of differences, as shown in Figure 16. Figure 16 was created using data from a calibration experiment where the MP particles (~350 μm PP

fragments) covered a large portion of the filter surface (Figure 17). This situation gave rise to the bimodal distribution shown. For environmental samples, it is not anticipated that MPs will make up such a high filter surface coverage as shown in Figure 17.

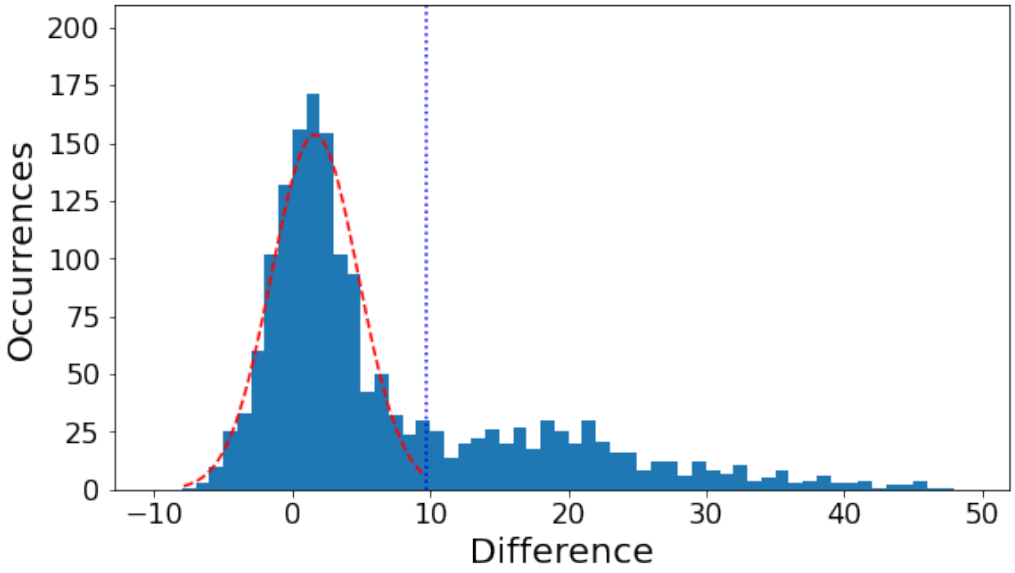

Figure 16. Histogram of reflectance differences (2750 cm^{-1} - 2850 cm^{-1}). Red Gaussian curve is fitted only to data below the vertical blue cutoff. Spectra above cutoff are considered to come from plastic particles. Cutoff is determined by 3Q+1.5IQR formula.

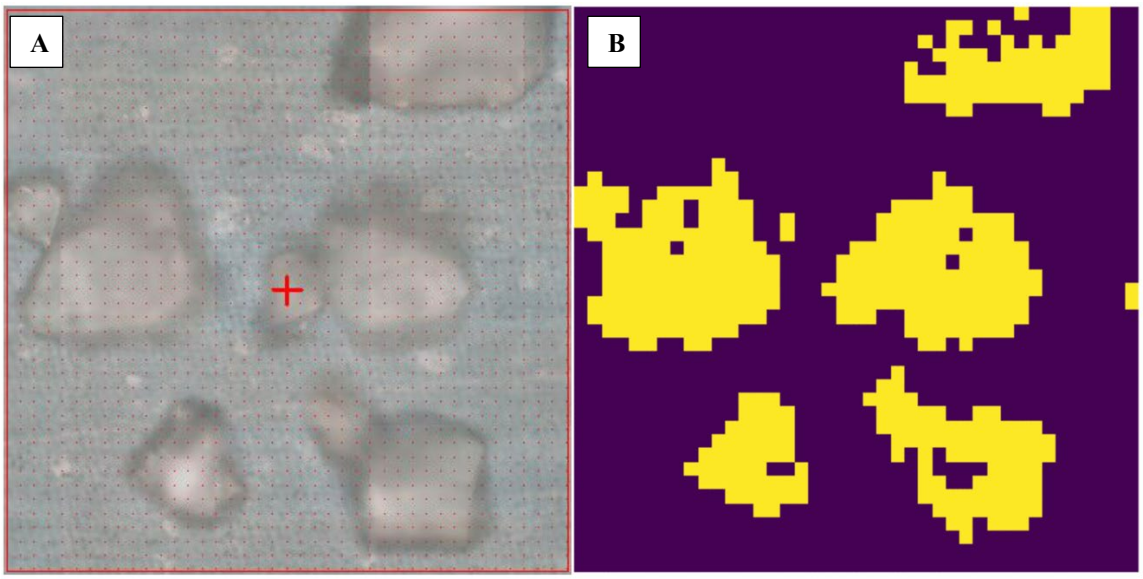

Figure 17. (A) Stitched visual image of 350 µm diameter PP particles on Anodisc filter. (B) Algorithm detected MP particles with predicted diameter of 432 µm.

The Python script was also capable of counting the number of MP particles it detected. Spectra from neighboring pixels, including diagonals, that were indicative of MP particles were assumed to be from the same particle, so one grouping of pixels, no matter how large, was always counted as one particle. The script was not capable of differentiating between overlapping particles. In such situations, overlapping particles were erroneously counted as the same particle. This situation can be seen in Figure 17 where two close particles are counted as the same particle. In Figure 17, the algorithm detected 8 particles. Of note is the fact that when the z-direction of the particle is too far from the surface of the filter, the spectral quality suffers immensely. This can be seen in Figure 17 where the centers of several of the larger particles do not register positively as MP particles because they are too far from the surface of the filter and the spectra from those locations was of poor quality. This essentially puts an upper limit of ~300 µm on the size of particles that can be evaluated with FTIR microscopy.

Similarly, the algorithm was not capable of detecting small individual MP particles that grouped together on the filter surface (Figure 18). The fact that the program counts diagonal pixels as the same particle reduces the number of detected particles in such cases. In these situations, the large "rafts" of particles are counted collectively as a single larger particle.

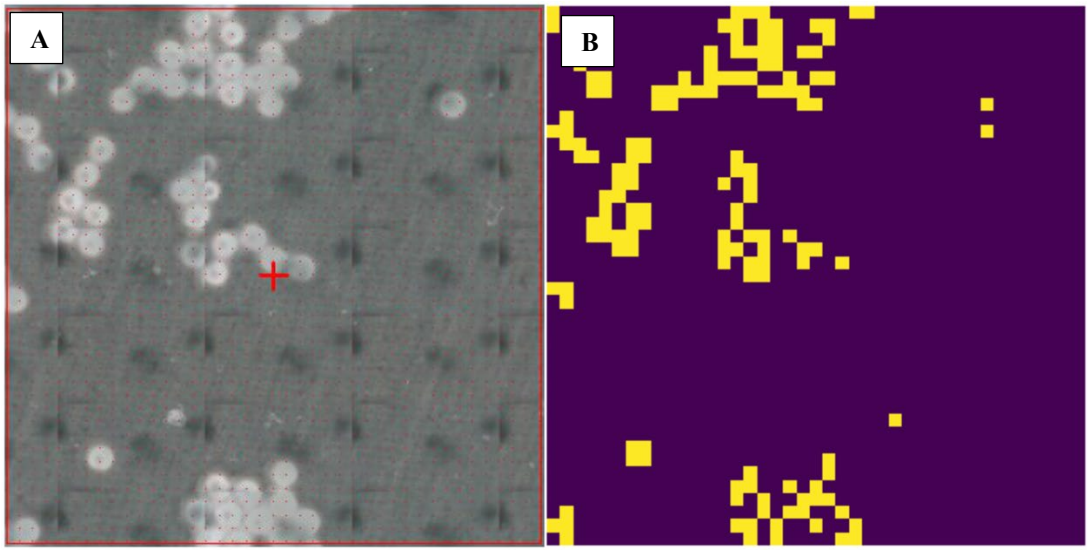

Figure 18. (A) Stitched visual image of 117 µm diameter PS microspheres on Anodisc filter. (B) Algorithm detected MP particles with predicted diameter of 166 µm.

Finally, the lower size limit for the algorithm was mainly determined by the step size of 50 µm. Because a step size of 50 µm is only able to reliably detect particles larger than 50 µm, the FTIR microscope was not able to obtain good quality spectra from particles smaller than 50 µm. Therefore particles <50 µm were not readily detectable by the program. For example, program was tested on a distribution of PE MP particles with a size distribution from 10-45 µm, and did a poor job detecting these smaller particles (Figure 19).

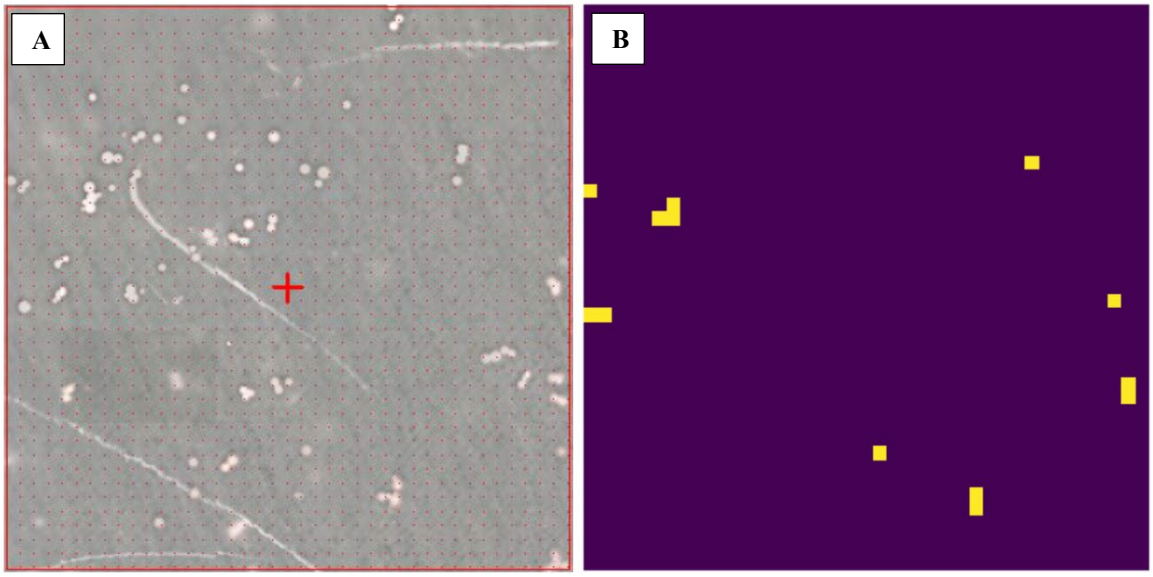

Figure 19. (A) Stitched visual image of 10-45 µm diameter PE particles on Anodisc filter. (B) Algorithm detected MP particles with predicted diameter of 71 µm.

The Python script was validated by analyzing 2x2 mm fields of view containing standard MP particles of known composition, size, and quantity. The standard particles that were used for the validation studies were 250 µm PVC fragments, 500 µm PP fragments, 117 µm PS spheres, 10-45 µm PE spheres, 300 µm PET fragments, 350 µm PE fragments, and 250 µm PS fragments. For each field of view, the number of particles was visually counted on the microscope view (e.g., (A) pane in Figures 17, 18, and 19) and algorithmically counted. A summary of the validation studies is shown in Table 3. The Python script also was programmed to show the average particle size based on an algorithm that assumed each particle to be circular. These algorithmically detected

particle sizes are shown in the rightmost column in Table 3. Overall, the counting algorithm performed admirably with all tested MP particles when compared to manual counting. The only notable exception to the performance of the counting program was its consideration of smaller particles that tended to "raft" together at higher concentrations, a condition that is not expected to occur in natural samples due to their more hydrophilic surface due to oxidative weathering. Nonetheless, in the calibration experiments, particle rafting led to algorithmic undercounting. These results support the simple assumption that the difference in absorbance between 2750 cm^{-1} and 2850 cm^{-1} is sufficient to uniquely identify MP particles on an Anodisc filter surface with reflectance FTIR microscopy.

Table 3. Python script validation summary.

Polymer	Shape	Visual Count	Program Count	Algorithmic Accuracy	Mfd. Size (μm)	Mean Diam. (μm)
PP	Fragments	8	8	100%	350	432
PVC	Fragments	16	14	87.5%	250	198
PET	Fragments	13	17	131%	300	128
PE	Fragments	12	10	83%	350	137
PE	Spheres	86	8	9%	10-45	71
PS	Fragments	12	16	133%	250	245
PS	Spheres	56	17	30%	117	166

CHAPTER 3: RESULTS AND DISCUSSION

3.1 Visual Microscopy Results

The morphological and quantitative results from the 333 – 4000 μm manta net samples are shown in Table 4. A total of 114 particles were detected from a total sampled surface area of 3.64×10^{-3} km^2. All four manta net ambient blanks yielded zero MP particles, indicative of non-detectable ambient MP contamination aboard the *R/V Blue Heron*. The most common particle morphology was fibers (50%), followed by fragments

(36%), films (5%), fiber bundles (4.5%), and foams (4.5%). MP fibers have previously been found to be the most abundant MP morphology in Lake Superior in a number of studies.[13,14,105] In a 2018 study utilizing 333 µm manta net sampling,[13] fibers were determined to make up 39% of recovered MP particles whereas a 2019 study of Lake Huron, Michigan, and Superior employing Niskin bottle sampling and 0.45 µm filtration, found fibers to make up >99% of recovered MP particles.[105] Similarly, a 2016 study of 29 Great Lakes tributaries using a 333 µm neuston net found fibers to make up 71% of all MP particles. Interestingly, a 2013 study of Lake Erie, Huron, and Superior surface waters using 333 µm manta nets found that "lines," a morphological proxy for fibers, made up less than 1% of all recovered MP particles.[14]

Table 4. Visual microscopy manta net summary.

Shape	Fiber	Fiber Bundle	Film	Foam	Fragment	Total	Concentration (MPs/km^2)
Station 4	13	1	0	2	16	32	21,000
Station 2	4	1	0	0	4	9	7,000
Station 7	18	0	0	1	4	23	49,000
Station 12	22	3	6	2	17	50	118,000
Total	57	5	6	5	41	114	-
Percent	50%	4.5%	5%	4.5%	36%	-	Mean: 48,750

The prevalence of fibers among Lake Superior MP particle morphologies in this study could be due to several factors. Firstly, MP fibers have been found to be readily transported in the atmosphere and have been found to be particularly abundant in urban air.[90] Thus, atmospheric deposition may be a significant source of MP fibers to Western Lake Superior. This is especially probable when considering the dominant atmospheric circulation in the area, the prevailing westerlies, and the leeward position of Lake Superior relative to the Twin Ports urban area (population 288,648). Another possible source of MP fibers to Lake Superior could be WWTP effluent. It has been shown that effluent from laundering synthetic fabrics in washing machines can lead to concentrations of >100 MP fibers per liter, or >1900 MP fibers per load.[91] The Western Lake Superior

Sanitary District (WLSSD) WWTP uses 1.7 mm anthracite coal, 0.55 mm silica sand, and several gravel sizes to filter all wastewater prior to discharge in the St. Louis River estuary, however, this filtration is not likely sufficient to remove all MP fibers from urban wastewater and in such a case, WWTP effluent could be a significant source of MP fibers to Lake Superior. In fact, a 2018 sampling campaign of the St. Louis River estuary found that the sampling location nearest to WLSSD had the highest concentration of MP particles with fibers being the most abundant morphology.[13] Finally, there is also evidence that MP fibers could be produced *in situ* in Lake Superior from other morphologies and sizes of plastic waste. *In vitro* research looking at the breakdown of plastic due to UV radiation and mechanical strain has shown that originally non-fibrous plastic morphologies such as films and thin sheets can break down to produce MP fibers.

When combined with the sampled surface area data from Table 1, the concentration of MP particles at each location is shown in the rightmost column of Table 4. Areal MP concentrations ranged from 7,000 to 118,000 particles per km^2. These results are the same order of magnitude as a previous study of Western Lake Superior surface waters that reported concentrations of 25,000 – 54,000 MP particles per km^2.[13]

Of the 114 particles that were visually detected via optical microscopy, 23 of those particles were large enough to be extracted from the MCE filter surface using metal forceps and were placed in glass vials for analysis via ATR-FTIR. Results from the ATR-FTIR analysis are shown in Table 5. The two particles that were unknown to the Hummel Polymer Library were uploaded to openspecy.org which reported that they were likely to be cellulose and therefore non-plastic. The ATR-FTIR results suggest that 9% of the 114 particles identified as MPs by visual microscopy are in fact non-plastic. In other words, the false positive rate by visual microscopy was 9%. Accordingly, it is likely that the total number of true MP particles captured by manta net (333 – 4000 μm) was closer to 104.

Table 5. Summary of particles collected by visual microscopy and subjected to ATR-FTIR validation.

Polymer	PE	PET	PP	Unknown	Total
Station 12	3	1	3	2	9
Station 2	1	1	0	0	2
Station 4	7	1	2	0	10
Station 7	0	2	0	0	2
Total	11	5	5	2	23
Percent	48%	22%	22%	8%	100%

Of all polymer types determined by ATR-FTIR, the predominance of PE (48%), PP (22%), and PET (22%) recovered from Western Lake Superior is in agreement with the fact that the majority of plastic that is produced worldwide is PE, PP, and PET.[1] 42% of all plastics produced is used for packaging, and plastic packaging is primarily PE, PP, and PET. It is worth mentioning that four of the five particles that were chemically characterized as PET were fibers. This result would seem to corroborate the idea that many fibers in Lake Superior are from synthetic polyester (PET) fabrics.

These results are also in agreement with a previous manta net survey in Western Lake Superior that found PE, PP, and PET to be abundant, as characterized by pyrolysis-GC/MS.[13] However, PVC is conspicuously absent in the current study results whereas previously it had been determined to be the most abundant polymer as characterized by pyrolysis-GC/MS.[13] This difference is notable given that the previous manta net survey and the current research both utilized saturated NaCl during sample processing, suggesting that the density separation procedure is not responsible for this discrepancy. The absence of PVC particles in the current study could be due to the low number of particles, only 23, that were chemically characterized by ATR-FTIR.

A 2019 study by Lenaker *et al.* used 333 µm neuston nets in Lake Michigan and analyzed 553 MP particles using FTIR spectroscopy.[101] In that study, 32% of FTIR-analyzed particles from surface waters were PP, 26% PS, and 20% PE. The fact that no PS was found in the current study suggests that the PS found by Lenaker *et al.* may be due to a contamination source that is local to the Milwaukee, WI metropolitan area. The high proportion of PS found in this study is aberrant when considering that PS only

makes up 7.6% of all polymer resins produced worldwide.[1] Furthermore, in the 2016-17 study of Western Lake Superior, only 2 of 42 particles investigated by py-GC/MS, or 4.7%, were determined to be PS.[13]

3.2 FTIR Microscopy Results

μFTIR results were analyzed both manually and computationally. The manual analysis (Table 6) relied upon visual inspection of the chemigram generated by OMNIC at 2850 cm^{-1}, as noted in the methods section. Computational analysis relied upon the difference between the absorbance at 2850 cm^{-1} and 2750 cm^{-1}. Of note, the Python script was written after every field of view had been manually analyzed, so in no way did it inform the initial manual analysis of the data. The Python script was used to check and validate the manual analysis, and vice versa. The results of this comparison (manual vs. algorithmic) highlighted the strengths and weaknesses of each approach.

Table 6. FTIR microscopy McLane pump summary.

Location	Sample Depth	Method	Size (μm)	Sample Volume (liters)	MPs	Concentration (MPs/m^3)
Station 4	0	Manta	>333	228225	32	0.14
	2	McLane	>100	102	144	1400
	26	McLane	>100	109.7	153	1400
Station 2	0	Manta	>333	183600	9	0.05
	2	McLane	>100	212	144	680
	26	McLane	>100	208.2	231	1100
	240	McLane	>100	204.3	82	400
Station 7	0	Manta	>333	70125	23	0.33
	2	McLane	>100	215.8	415	1900
	18	McLane	>100	212	134	630
Station 12	0	Manta	>333	63750	50	0.78
	2	McLane	>100	212	72	340
	18	McLane	>100	215.8	53	240
Western Mooring	2	McLane	>100	215.8	440	2000
Method Blank	-	McLane	-	-	0	0

3.2.1 µFTIR Manual Analysis

Results from the manual analysis of the µFTIR data are shown in Table 6. Particle concentrations ranged from 240 MPs per m^3 at the 18-meter depth from Station 12 to 2000 MPs per m^3 at the western mooring subsurface. Interestingly, the western mooring was the most remote location sampled, yet yielded the highest number of subsurface MPs collected with the McLane pump. Unfortunately, a CTD water column profile was not obtained from this location during sampling. Station 2 had the most stratified water column of all stations sampled, with a well-defined chlorophyll maximum and thermocline, indicative of strong stratification (Figure 20).

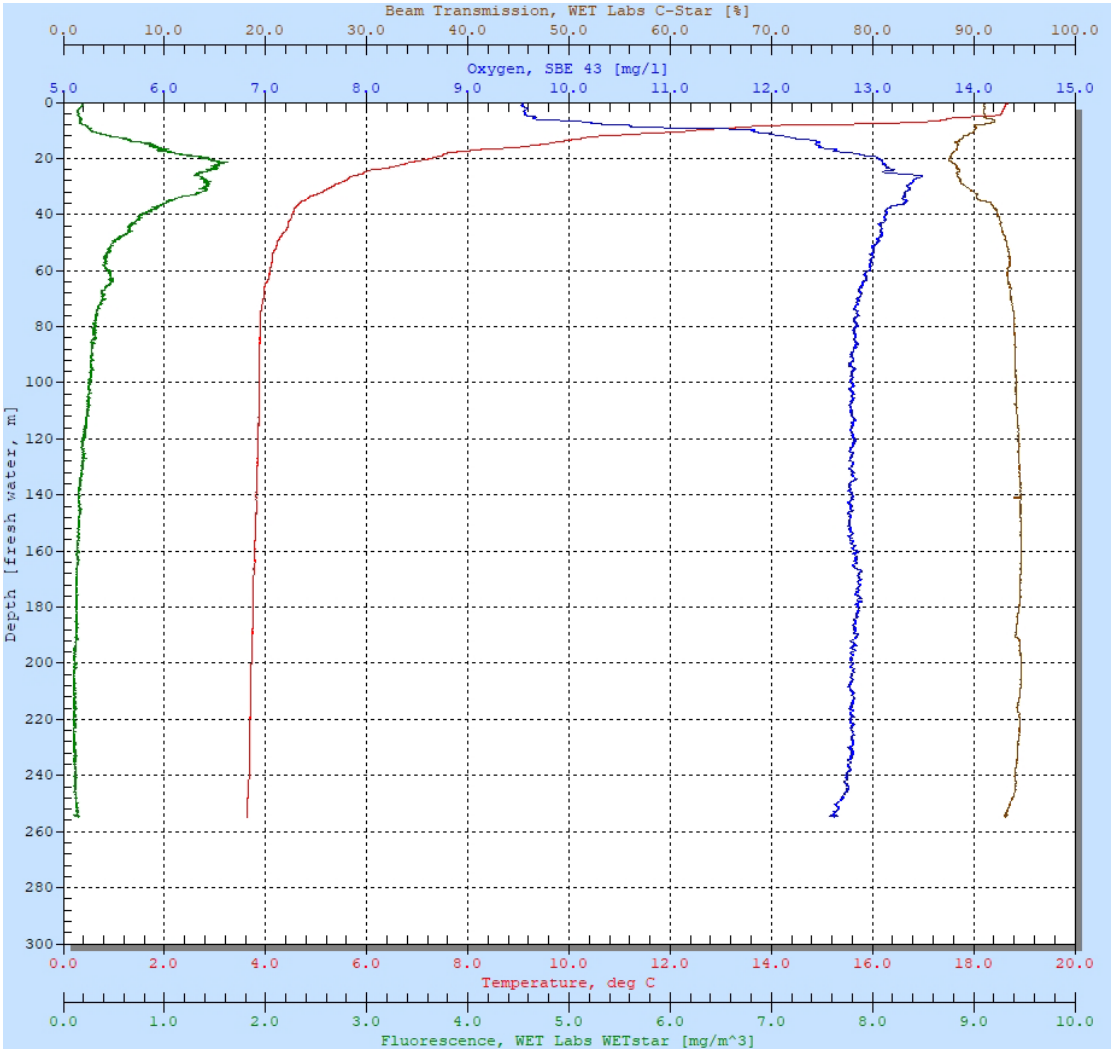

Figure 20. Vertical profile of fluorescence, oxygen concentration, temperature, and beam transmission at station 2. Green (fluorescence, mg/m^3), red (temperature, °C), blue (oxygen, mg/l), brown (beam transmission, %).

Because of the water column stratification, station 2 was the only station where our hypothesis could be appropriately tested. Although only one station, the data from station 2 support our hypothesis that MP particles should concentrate at the depth of the chlorophyll maximum and the pycnocline. The dense 4 °C water below the chlorophyll maximum acts as a barrier through which lighter particles will not settle, including lighter MP particles. Therefore, the particles will aggregate at the level of the chlorophyll maximum. At station 2, the subsurface concentration of MP particles was 680 MPs/m^3, the chlorophyll max concentration of MP particles was 1,100 MPs/m^3, and the hypolimnion concentration of MP particles was 400 MPs/m^3 (Figure 21). It is interesting to note that at station 2 there was no noticeable beam extinction at 240 meters (Figure 20) ruling out the presence of a Benthic Nepheloid Layer. The absence of a BNL is in accordance with the low calculated MP particle concentration from this depth. It is likely that MP particles that settle to this hypolimnetic depth simply continue their downward journey and incorporate into benthic sediments as there is no physical reason for them to be found in the hypolimnion in the absence of a BNL.

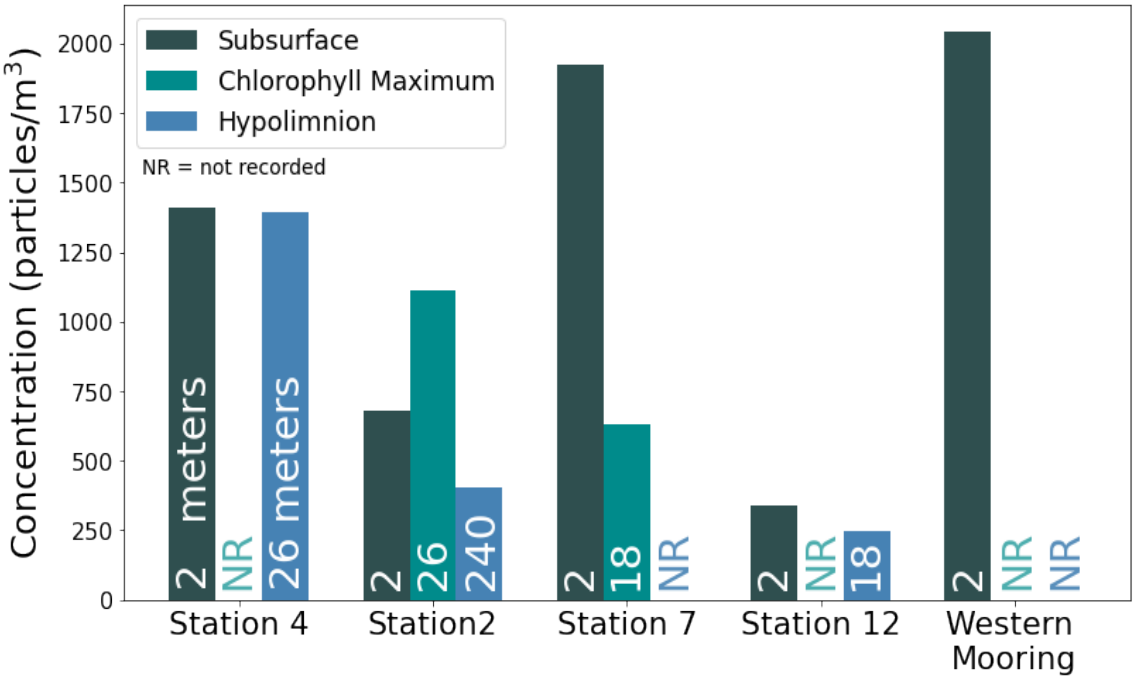

Figure 21. Calculated MP particle concentrations in Western Lake Superior. Note, chlorophyll maxima were only present at stations 2 and 7.

Station 4 was the only sampling location where a BNL was identified by the beam transmissometer, as indicated by decreased beam transmission beginning around 24 meters (Figure 22). As expected, among all samples collected from the hypolimnion, the concentration of MP particles collected from the BNL at station 4 was the highest at 1400 MPs/m^3. BNLs may have been present at the other sampling stations, however the BNL at station 4 was the only one identified by the beam transmissometer on the CTD rosette. The presence of significant concentrations of MP particles within the BNL at station 4 suggests that Lake Superior sediments may be a significant sink for MP particles.

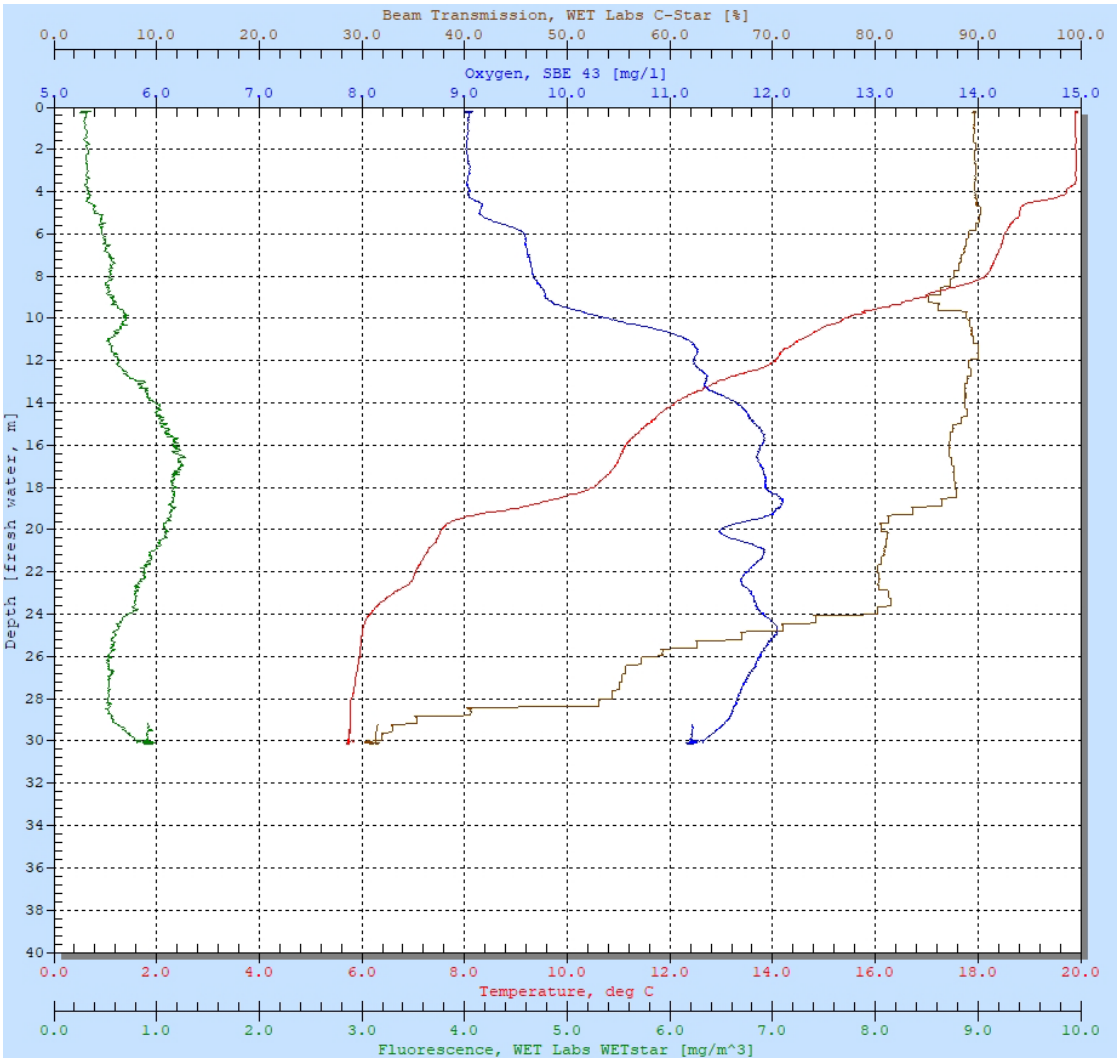

Figure 22. Vertical profile of fluorescence, oxygen concentration, temperature, and beam transmission at station 4. Green (fluorescence, mg/m^3), red (temperature, °C), blue (oxygen, mg/l), brown (beam transmission, %).

Apart from station 2, station 7 was the only other location where a chlorophyll maximum was identified. However, the station 7 chlorophyll maximum did not coincide with a significant decrease in beam transmission (Figure 23) as was the case at station 2. This may be a reason why a greater concentration of MP particles was not detected at the depth of the chlorophyll maximum. That is, it may be that a marked decrease in beam transmission, as was observed at the station 2 chlorophyll maximum, is required in addition to a defined chlorophyll to better predict the presence of microplastics.

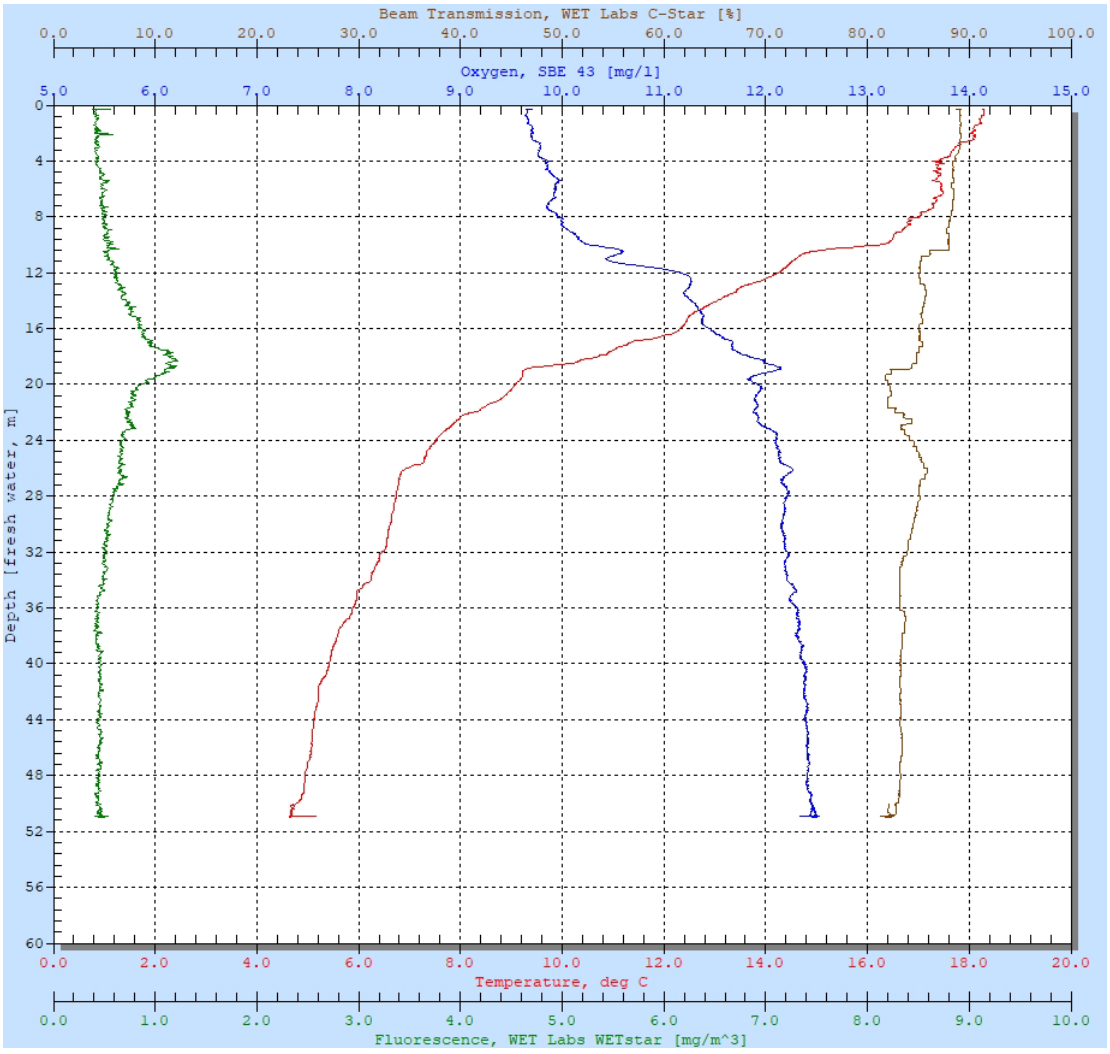

Figure 23. Vertical profile of fluorescence, oxygen concentration, temperature, and beam transmission at station 7. Green (fluorescence, mg/m^3), red (temperature, °C), blue (oxygen, mg/l), brown (beam transmission, %).

Overall, except for station 2, the greatest concentration of MPs at each station was found at a depth of two meters. Across all stations, excepting station 2, the average MP concentration at the subsurface was 1430 ± 780 MPs/m^3 (mean ± sample standard deviation) whereas the average MP concentration for all other water column samples was only 760 ± 590 MPs/m^3. This difference, however, was not statistically significant ($p = 0.27$) based on a one-way ANOVA after Shapiro-Wilk tests for normality (both $p > 0.05$) and a Levene test for equality of variances ($p = 0.65$). Although not statistically significant, this result suggests that in the absence of a well-structured water column, the greatest concentration of MPs may be found at or near the surface.

The method blank that was carried forward through the entire processing protocol yielded zero MP particles by manual analysis of the μFTIR data. Therefore, none of the particle concentrations in Table 6 were corrected or adjusted in any way. The method blank yielding zero MP particles is indicative of good protocols for cleanliness such as only wearing cotton lab coats, covering all sample containers with aluminum foil, using only Milli-Q water, and combusting NaCl before use to ensure the volatilization of any possible plastic contaminants. The computational analysis of the same method blank is discussed below.

Table 6 includes data from the manta net in the rightmost column, reported as particles per unit volume. The manta net data can be reported volumetrically because the net is designed to sample the top 15 cm of the water column. Therefore, the volume of sampled water can be calculated and the concentration per unit volume can be determined in addition to the concentration per unit area, as previously discussed. The surface MP concentrations calculated from the manta net data are notably lower than the McLane pump concentrations by approximately three orders of magnitude. The massive difference between the two sampling techniques could be due to several factors.

As mentioned previously, it has been widely observed that environmental plastic concentrations are inversely proportional to particle size.[97] According to this established trend, it is not surprising that the concentration of >100 μm particles collected by the McLane pump is higher than the concentration of >333 μm particles collected by the manta net. For example, if the breakdown of plastics in Lake Superior obeys an inverse third order power law, then the number of 100 μm MPs would be 36.9 times greater than

the number of 333 µm MPs.[8] However, our data show that the average number of 100 µm MPs (1020 ± 660 MPs/m^3) is 3,090 times greater than the average number of 333 µm MPs (0.33 ± 0.33 MPs/m^3). This is almost two orders of magnitude larger than what we would expect if we assumed an inverse third order power law to govern the distribution of MPs in Western Lake Superior.

Notably, in a study of the size distribution of plastic particles weathered by UV radiation and subjected to mechanical abrasion, Song *et al.* found relationships up to the order of inverse 4.5 for PP and expanded PS.[15] If an inverse 4.5 order relationship is assumed for Western Lake Superior, then 100 µm MPs would be 224 times more abundant than 333 µm MPs. Under such assumptions, the current data are still off by approximately one order of magnitude. As it stands, the data obtained in this study obey an inverse 6.68 order power law, based on two datapoints. Other factors that are undoubtedly contributing to the vastly different particle counts between 100 µm MPs and 333 µm MPs are the mode of sampling and the mode of analysis.

Regarding the modes of sampling, the 100 µm MPs were collected with the McLane pump and the 333 µm MPs were collected with the manta net and this inherently limits the comparability of the two size ranges. A particularly glaring difference between the two sampling methods was the volume of water sampled by each technique. On average, the manta net sampled 136,425 ± 71,292 liters per cast whereas the McLane pump only sampled 190.8 ± 42.6 liters per cast. Previous research has specifically compared manta trawls with *in situ* pumping methods and concluded that as long as a sufficient volume of water is filtered, both techniques are suitable for MP research.[63] It is also worth mentioning that because the McLane pump actively records pumping volumes with an inboard flow meter, the calculated volumes are very precise and accurate. With the manta net, winds, waves, and currents can influence the mounted flow meter and choppy waters can influence the depth of water that flows through the net. For all these reasons, the calculated volumes for the manta net are presumed to be less accurate and less precise.

In this research, the difference in calculated concentration for 100 µm MPs and 333 µm MPs was also likely influenced by the mode of sample analysis. The 100 µm MPs were analyzed using µFTIR and the 333 µm MPs were analyzed using visual

microscopy. A likely source of error during μFTIR analysis of the McLane pump samples was the counting of small bits of organic matter - matter that escaped oxidation - as MP particles. Although oxidations were carried out until no more organic matter was visibly present in the reaction vessel, it is likely that some very small, non-visible organic matter particles were able to escape complete oxidation and were filtered onto the Anodisc filters that were subsequently analyzed with μFTIR spectroscopy. Because our technique utilized the sp^3 C-H stretch as the primary indicator of a MP particle, our analytical approach cannot tolerate any organic matter alongside MPs particles on the Anodisc filter. However, visual inspection of the Anodisc filters showed that such organic matter contamination did indeed occur as evidenced by the presence of brown particles with visible cellular structures. This is likely to be a primary reason why MP particle counts from the μFTIR analysis are so high compared to MP particle counts determined by visual microscopy. Unfortunately, incomplete oxidation may have led to the breakdown of larger organic matter particle into many smaller organic matter particles that were then erroneously counted as that many individual MPs. A specific understanding of how Lake Superior organic matter reacts during the oxidation protocol would provide invaluable information to guide future oxidation protocols. Perhaps longer oxidation incubation periods are necessary in the future to minimize the amount of organic matter contamination.

In a similar vein, MPs in the manta net samples that were analyzed by visual microscopy were prone to several detection issues that may have led to particle misidentification and inaccurate particle counts. For example, clear plastics are commonly undercounted when analyzing MP samples.[76] This may have contributed to the low particle concentrations for the manta net samples as shown in Table 6. The manta net samples were also very contaminated samples to begin with, containing bird feathers, algae, and other organic matter. While the oxidation step removed the largest of these contaminating agents, it was very clear that some non-MP material remained in the sample after oxidation. This material may have covered up some MP particles making them impossible to detect by optical microscopy. In Figure 24, the golden material behind the green PE MP is incompletely oxidized organic matter or very fine clay that

could have contributed to "burying" MP particles on the gridded MCE filters that were used for optical microscopy analysis.

Figure 24. Green PE MP on MCE filter with residual non-oxidized organic matter, as observed by visual microscopy.

As mentioned previously, in studies using chemical analytical methods to validate the performance of optical microscopy MP identification, misidentification rates are reported to be between 9% and 98%.[76] In this study, 9% or two of 23 suspected MP particles that were subjected to compositional analysis were determined to be cellulosic material (i.e., non-plastic). Accordingly, this research had a misidentification rate on the lower end of the spectrum of misidentification rates reported in the literature. This research subjected 23 of 114 visually identified particles to ATR-FTIR validation studies. Thus, approximately 20% of suspected MP particles were tested to confirm the accuracy of the visual identification protocol used, greater than the recommended 5-10%.[111]

When comparing the vertical distribution of open water MPs in Western Lake Superior (Table 6) to the only other open water vertical distribution reported for the Great Lakes - characterized just outside the Milwaukee harbor - there are several notable differences. Outside the Milwaukee harbor, at five depths (0-13.7 meters), sampling with a 333 µm net, and across four different sampling excursions, MP particle concentrations were all consistently less than 2.5 particles per m^3.[101] While subsurface MP concentrations in this study were all several orders of magnitude larger (1020 ± 660 MPs/m^3) than the subsurface concentrations outside the Milwaukee harbor, it is important to note that our subsurface concentrations were for particles >100 µm as opposed to >333

μm. As mentioned above, this size difference could be accounted for by the fact that smaller MP particles are expected to be more abundant. It is especially interesting to note that our surface MP concentrations (0.33 ± 0.33 MPs/m^3) are in excellent agreement with the surface concentrations reported just outside the Milwaukee harbor (0.42 MPs/m^3).[101] This is notable because both studies used the same 333 μm mesh size for sampling. The data from Lake Michigan yielded no clear trends in the vertical distribution of MPs. Similarly, apart from station 2 in our study aligning with our hypothesis of increased MP concentrations at the chlorophyll maximum, there was no statistically significant trend in our data. In our study, the number of MPs at the surface was also lesser by several orders of magnitude but was clearly influenced by the sampling mode and the fact that the surface was sampled with a larger mesh size.

Although not within the Great Lakes, a 2021 study from the Canary Islands looked at the vertical distribution of MP particles from the sea surface down to 1150 m.[112] Importantly, this study used 100 μm filters to collect samples and found that in the winter of 2019, MP fragments and fibers in the water column were present in concentrations ranging from 100 to 3,000 particles per m^3. In the autumn of 2019, MP fragments and fibers were present in concentrations ranging from 1,000 to 90,000 particles per m^3. These >100 μm MP concentrations are notable, particularly the winter concentrations, because they are on the same order of magnitude as the water column MP concentrations determined in this research (Table 6). The notable differences between the current research and the Canary Islands study are the sampling technique (*in situ* McLane pumping vs. Niskin bottle volume sampling, respectively), the water sampled (freshwater lake vs saltwater ocean), and the mode of analysis (μFTIR spectroscopy vs. optical microscopy). Interestingly, the Canary Islands study found that high zooplankton abundance was positively correlated with high MP concentrations. In our investigation of MP abundance as a function of water column depth, we did not attempt to relate MP concentration to zooplankton abundance. However, we did explore whether chlorophyll presence influenced MP abundance and at station 2, the station with the most well-defined chlorophyll maximum, this hypothesis was confirmed. However, further validation of this hypothesis will require much more sampling of strongly stratified Lake Superior water columns.

Another 2020 paper looked at the vertical distribution of MPs at various depths throughout the water column in the Arctic Ocean and found concentrations to be 161 ± 293 MP/m^3, within the same order of magnitude as the 1020 ± 660 MPs/m^3 found in this research.[106] The Arctic study is worthy of mention in this context because similar to the current research, samples were analyzed using an automated data analysis pipeline and μFTIR spectroscopy, albeit with a Focal Plane Array (FPA) detector that significantly expedited analysis. Additionally, exactly like the current research, MP concentrations in the Arctic Ocean were found to be highest in the near surface samples (1-meter depth) at all but one of the five stations sampled. Interestingly, the exception in both studies was at the deepest station sampled, where the highest MP concentration was deeper in the water column, 26 meters in the current study and 5350 meters in the Arctic.

3.2.2 μFTIR Computational Analysis

Results from the computational analysis of the 100 μm McLane pump filters are shown in Table 7 and Figure 25. On average, the detection algorithm yielded a concentration of 3040 ± 1340 MPs/m^3, approximately three times the concentration found by visual analysis of the μFTIR data (1020 ± 660 MPs/m^3). Very notably, the algorithm successfully detected 78% of all the particles that were detected visually. Despite the high number of particles detected by the algorithm overall, the 78% success rate is still an impressive result for a detection algorithm based on nothing more than the difference in reflectance between 2750 cm^{-1} and 2850 cm^{-1} due to poor spectral quality. The individual particles that were detected both visually and algorithmically (light blue, Figure 25) is perhaps the best subset of particles to use to calculate the final concentration of MP particles. Using this intersection of visually identified particles and algorithmically detected particles, the concentration of MPs in Western Lake Superior can be calculated as 760 ± 570 MPs/m^3. The automatic analysis of the McLane method blank identified a concentration of 140 MPs/m^3, significantly more than the manual analysis which identified zero MP particles. This is likely an artifact of the algorithm that determines outliers (as discussed below) because the 140 MPs/m^3 concentration was identified on a blank filter. Therefore, it could be used to correct the other concentrations to account for the algorithmic error. The data in Table 7, however, have not been corrected as described.

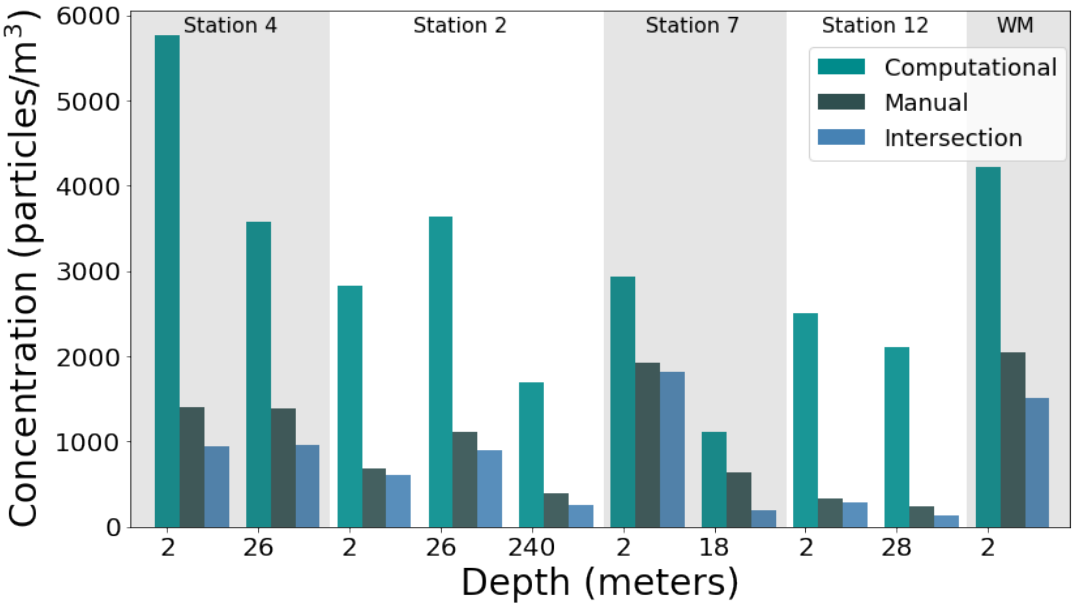

Figure 25. Comparison of computational and manual analysis of µFTIR data.

Table 7. Computational analysis summary and comparison to manual analysis.

Station	Depth (m)	Computer Conc. (MPs/m^3)	Manual Conc. (MPs/m^3)	Intersection Conc. (MPs/m^3)	Average Particle Size (µm)	Computer Accuracy
4	2	5770	1400	940	73	0.67
4	26	3600	1400	960	85	0.69
2	2	2830	680	610	82	0.90
2	26	3630	1100	900	83	0.81
2	240	1700	400	260	74	0.65
7	2	2940	1900	1800	104	0.94
7	18	1100	630	200	63	0.32
12	2	2500	340	290	66	0.87
12	18	2100	240	100	62	0.55
WM[1]	2	4210	2000	1500	74	0.74
Method Blank	NA	140	0	0	60	0
Mean[2]	NA	3040	1020	760	77	0.78[3]
Std. dev.[2]	NA	1340	660	570	13	0.19

[1] Western Mooring
[2] Excludes Blank
[3] Weighted Average

The results displayed in Figure 25 are primarily notable for the fact that the intra-station trends for the computational analysis are almost identical to the intra-station trends for the manual analysis. The only exception to the agreement in trends between the two analytical approaches is station 4. At station 4, the manual analysis yielded equal MP concentrations at the subsurface and at 26 meters, whereas the computational analysis yielded a significantly higher MP concentration at the subsurface. The concordance of trends between the computational and manual analytical approaches (and their intersection) is important because it shows that the computational pipeline could distinguish relative differences in MP concentrations at each station. The agreement in trends is also important because the computationally determined trends can corroborate the conclusions that were made based on the manually determined trends in the preceding section. For example, at station 2 where the chlorophyll maximum was well-defined, the concentration of MP particles identified by the algorithm was highest at the depth of the chlorophyll maximum. In summary, while both analytical approaches yielded similar trends, the MP concentrations identified by the computational approach were significantly higher.

A likely cause of the high number of particles detected by the algorithm is the fact that the computational criteria for a MP particle is based on the formula for a high outlier, $Q3 + 1.5 \times IQR$, and this formula is too liberal in its determination of outliers. If the IQR was multiplied by a factor greater than 1.5, the formula would be stricter, and the number of particles detected by the algorithm would be appropriately reduced. For example, Figure 26 shows the histogram of differences for the eighth field of view on the station 4 filter that was collected from the subsurface. In this figure, the differences to the immediate right of the vertical blue dotted line are counted as outliers and therefore as MP particles. For this field of view, the algorithm detected 18 particles whereas visual analysis only yielded three particles. If the formula for outliers was stricter, then the blue cutoff line would move farther to the right and the algorithm would detect fewer particles. Altering the detection algorithm in this manner would likely improve the agreement between visual detection and computational detection.

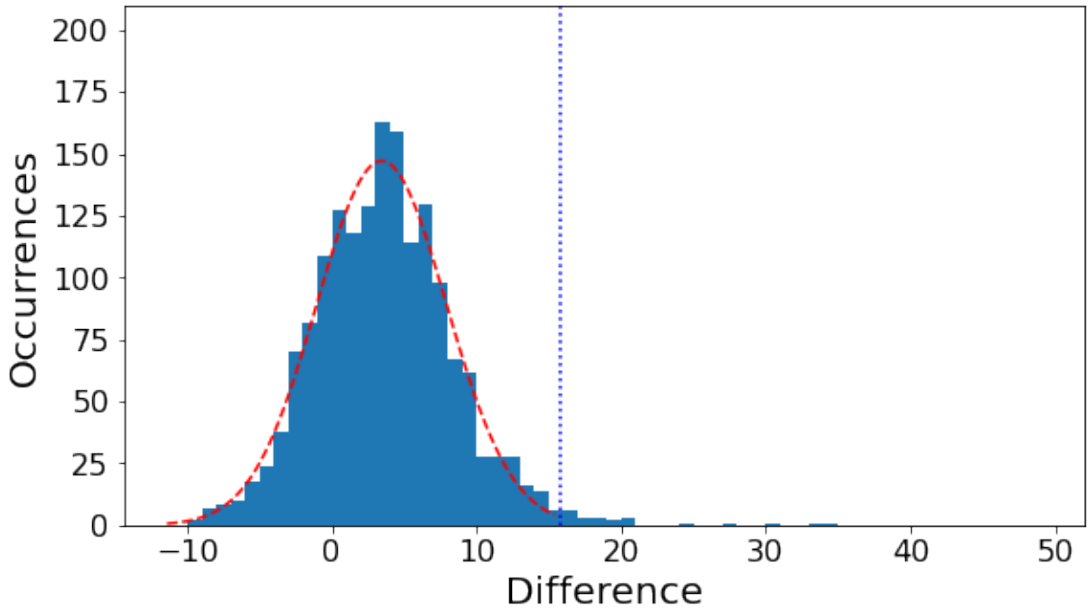

Figure 26. Histogram of reflectance differences (2750 cm^{-1} - 2850 cm^{-1}). Station 4, 2-meter depth, field of view #8. Red Gaussian curve is fitted only to data below the vertical blue cutoff. Spectra above cutoff are considered to come from plastic particles. Cutoff is determined by 3Q+1.5IQR formula.

Another important consideration when interpreting the results of the computational analysis is the fact that the algorithm is based on a crude difference in reflectance (2750 cm^{-1} - 2850 cm^{-1}), not on spectral matching. Replacing the current algorithm with spectral matching functionality in the analytical pipeline would be the best way to improve the results of the program. This, however, was not possible because the spectral quality from the µFTIR spectrometer was not suitable for comparison with database-quality spectra. The development of the reflectance-difference based algorithm was simply a response to the limitation of poor spectral quality. If spectral quality was improved, for example by utilizing a FPA or by performing transmission experiments rather than reflectance experiments, the current program could be easily amended to include a spectral matching functionality. In such a case, polymer type would be another variable collected by the program. However, until spectral quality improves, the algorithm as it currently stands is perhaps best utilized as a pre-analytical screening tool that can recommend pixels (spectra) on a chemigram that are likely to be MP particles. A researcher can then manually verify whether these spectra represent MPs. This would be beneficial because rather than searching through ~1700 spectra per field of view, the

researcher would now only have to analyze the pixels that were suggested by the algorithm. Because the program was written after all μFTIR data had been visually analyzed, this recommendation-based approach was not realized in the current research. In its current state, the algorithm could additionally be used as a pre-screening tool prior to spectral matching approaches. That is, subjecting all spectra from one field of view to library searches could be prohibitively time intensive unless a quick pre-screening algorithm, such as the one presented here, was used to recommend spectral candidates that were likely to yield positive hits when compared with a full spectral library.

The implementation of the Python MP detection algorithm herein was inspired by the desire to build a completely automated analysis pipeline capable of determining counts and average sizes of MPs extracted from aquatic environmental matrices. Because typical MP research often requires laborious counting protocols, the development of such automated pipelines for MP analysis is highly desirable to improve standardization between labs, increase throughput, and reduce time spent performing repetitive identification tasks. After all, repetitive tasks are among those most amenable to automation. The pipeline in this research, though lacking a robust spectral matching functionality, is notable for being one of the few completely automatic pipelines to successfully analyze samples that were collected from the environment.

It is also important to note that the challenge of collecting quality μFTIR spectra from MP-containing natural samples is by no means a challenge unique to this research. Spectrometer settings, spectrometer brand, filter material, and time constraints are among the many factors that need to be considered that influence spectral quality.[76] A broadly applicable approach to achieve excellent μFTIR spectra has yet to be expounded. While good results have been achieved by individual laboratories with specific spectrometers and software,[74,87] such instrumentation is far from being universally available. Furthermore, many proposed detection methodologies offer nothing more than proof of concept. Such methodologies either demonstrate the detection of manufactured MPs on otherwise clean filters[74] or the detection of manufactured MPs that were added to natural sediment samples.[85] Proof of concept is important, yet there is a wide gulf between the challenge of detecting primary MP particles on clean filters and the challenge of detecting secondary MP particles that have been weathered, biofouled, and degraded and

are present alongside sediment, natural organic matter, and other confounding materials. Considering this, the analytical pipeline described in this research is notable for being tolerant of subpar spectral quality as well as its capacity to detect MP particles contained within natural samples.

Previous efforts to automate the analysis of MP particles in environmental matrices have varied in their objectives. One of the most comprehensive MP data analysis pipelines was introduced by Primpke *et al* in 2017.[87] The pipeline described in this work made use of IR spectra gathered using a FPA detector followed by image analysis with the Simple ITK image processing module in Python and comparison of all spectra to a reference database. This methodological pipeline is notable because it is capable of detecting MPs that were gathered from a variety of environmental media, whereas many methodology papers present proof of concept without testing the concept on environmental samples.[74] This pipeline has been used in several projects since that time.[95,106] A similar software package called siMPle (Systematic Identification of MicroPLastics in the Environment), has also been made available for download online. Unfortunately, the spectra gathered in this research were not of sufficient quality to be compatible with this software. This incompatibility led to the development of the novel Python script as discussed above. The siMPle software (previously known as MPHunter) has been used successfully several research groups to identify MPs in environmental matrices.[113] Another version of automated MP detection focused on classifying the morphologies of particles already known to be MPs.[114]

CHAPTER 4: FUTURE WORK

The research presented herein could be augmented on multiple fronts. Regarding sampling, more water volume is always desirable as it reduces statistical errors when extrapolating results.[63] To this end, future MP sampling cruises on Lake Superior would do well to increase the volume sampled by the McLane pumps. In this research, a maximum of ~200 liters were filtered, however with the available McLane pumps, volumes as large as 4,000 liters can be sampled with one cast. Similarly, to get better synchronicity of results between different size ranges, it is preferable that different size

ranges are collected with the same sampling method. Because dragging manta nets with different mesh sizes in series is not possible (not to mention that manta nets smaller than 333 μm create too much drag to be feasible), different mesh size filters should be placed in the filtration manifold of the McLane pumps. Given the height of the filtration manifold on the McLane pump, it is theoretically possible to place many filter sizes serially, perhaps as many as four or five. Such an experimental set up would allow for more appropriate comparability of results from different size ranges as the mode of sampling would be controlled. Additionally, the McLane pump is advantageous because it can be deployed at multiple depths whereas manta nets are restricted to surface sampling.

Regarding sample processing, more information should be gathered about the thoroughness of the oxidation process with Fenton's reagent. Such information is necessary so that the process can be amended if necessary to ensure complete oxidation of all organic matter. The current μFTIR data analysis approach relies on the assumption that 100% of the organic matter is oxidized during processing, so it would be prudent to assay the efficacy of the oxidation process to confirm that this assumption is appropriate.

Concerning the prevalence of MP fibers in Lake Superior waters, further directed research is necessary to better understand their most likely source. Longitudinal sampling of waters directly near WWTP effluent discharge sites, such as near the WLSSD WWTP, would do much to elucidate the potential role that WWTPs play in discharging MP fibers into Lake Superior. Controlled *in situ* studies of plastic degradation in Lake Superior would show whether common plastic waste morphologies tend to break down into MP fibers. Similarly, controlled wet and dry atmospheric deposition studies are necessary to clarify whether atmospheric transport is a significant source of MP fibers to Western Lake Superior.

Without a doubt, the greatest challenge of this research project was to obtain good quality IR spectra from small MP particles interspersed with suspended sedimentary material on an uneven aluminum oxide filter surface. Unfortunately, this remained a recalcitrant challenge and was not wholly overcome during this research project. Nonetheless, this challenge also represents perhaps the greatest opportunity to improve the current research. That is, by obtaining better quality IR spectra, a matching algorithm

could be implemented into the existing analytical pipeline which would significantly enhance the quality and confidence of the algorithmic results. There are at least two known avenues that could be followed in the pursuit of better IR spectral quality. First, finding an effective method to keep the aluminum oxide filter uniformly flat on the microscope stage would preclude spectral distortions caused by an inconsistent depth of focus. Second, performing transmission experiments in place of reflectance experiments would increase the interaction of IR radiation with the sample and possibly greatly improve spectral quality. If transmission experiments improve spectral quality enough, it may not be necessary to find a method to flatten filters uniformly, as discussed above. Additionally, background handling for transmission experiments is much more accurate than for reflectance experiments.

Overall, the current research has laid the groundwork for future studies to look at the size distribution of MPs in Lake Superior as well as the vertical distribution of MPs throughout the water column. The improved characterization of both the size distribution and the spatial distribution will be integral to understanding how MPs behave in Lake Superior and determining their ultimate sink. Additionally, this work has made important first steps towards the completely automated analysis of MP particles contained in environmental matrices. Improvements to the current analytical pipeline will enable better reproducibility and improve throughput which will in turn will permit the initiation of reliable long term MP monitoring programs in Lake Superior and other lentic aqueous systems.

REFERENCES

1. Geyer, R., Jambeck, J. R. & Law, K. L. Production, use, and fate of all plastics ever made. *Sci. Adv.* **3**, 25–29 (2017).
2. Lebreton, L. & Andrady, A. Future scenarios of global plastic waste generation and disposal. *Palgrave Commun.* **5**, 1–11 (2019).
3. Cherif Lahimer, M., Ayed, N., Horriche, J. & Belgaied, S. Characterization of plastic packaging additives: Food contact, stability and toxicity. *Arab. J. Chem.* **10**, S1938–S1954 (2017).
4. Luijsterburg, B. & Goossens, H. Assessment of plastic packaging waste: Material origin, methods, properties. *Resour. Conserv. Recycl.* (2014) doi:10.1016/j.resconrec.2013.10.010.
5. D'ambrières, W. Plastics recycling worldwide: Current overview and desirable changes. *F. Actions Sci. Rep.* **2019**, 12–21 (2019).
6. Hoegh-Guldberg, O. *et al.* Plastic waste inputs from land into the ocean. *Science (80-.).* 1655–1734 (2015) doi:10.1017/CBO9781107415386.010.
7. Ryan, P. G., Turra, A. & Kershaw, P. J. GESAMP 2019 Guidelines for the monitoring & assessment of plastic litter in the ocean Reports & Studies 99 (editors Kershaw, P.J., Turra, A. and Galgani, F.). **99**, (2019).
8. Cózar, A. *et al.* Plastic debris in the open ocean. *Proc. Natl. Acad. Sci. U. S. A.* **111**, 10239–10244 (2014).
9. Law, K. L. *et al.* Plastic accumulation in the North Atlantic subtropical gyre. *Science (80-.).* **329**, 1185–1188 (2010).
10. Ter Halle, A. *et al.* Understanding the Fragmentation Pattern of Marine Plastic Debris. *Environ. Sci. Technol.* **50**, 5668–5675 (2016).
11. Eriksen, M. *et al.* Plastic Pollution in the World's Oceans: More than 5 Trillion Plastic Pieces Weighing over 250,000 Tons Afloat at Sea. *PLoS One* **9**, 1–15 (2014).
12. Villarrubia-Gómez, P., Cornell, S. E. & Fabres, J. Marine plastic pollution as a planetary boundary threat – The drifting piece in the sustainability puzzle. *Mar. Policy* **96**, 213–220 (2018).
13. Hendrickson, E., Minor, E. C. & Schreiner, K. Microplastic Abundance and Composition in Western Lake Superior As Determined via Microscopy, Pyr-GC/MS, and FTIR. *Environ. Sci. Technol.* **52**, 1787–1796 (2018).
14. Eriksen, M. *et al.* Microplastic pollution in the surface waters of the Laurentian Great Lakes. *Mar. Pollut. Bull.* **77**, 177–182 (2013).
15. Song, Y. K. *et al.* Combined Effects of UV Exposure Duration and Mechanical Abrasion on Microplastic Fragmentation by Polymer Type. *Environ. Sci. Technol.* **51**, 4368–4376 (2017).
16. Jahnke, A. *et al.* Reducing Uncertainty and Confronting Ignorance about the Possible Impacts of Weathering Plastic in the Marine Environment. *Environ. Sci. Technol. Lett.* **4**, 85–90 (2017).
17. Gewert, B., Plassmann, M. M. & Macleod, M. Pathways for degradation of plastic polymers floating in the marine environment. *Environ. Sci. Process. Impacts* **17**, 1513–1521 (2015).
18. François-Heude, A., Richaud, E., Desnoux, E. & Colin, X. A general kinetic model

for the photothermal oxidation of polypropylene. *J. Photochem. Photobiol. A Chem.* **296**, 48–65 (2015).
19. Andrady, A. L., Pegram, J. E. & Song, Y. Studies on enhanced degradable plastics. II. Weathering of enhanced photodegradable polyethylenes under marine and freshwater floating exposure. *J. Environ. Polym. Degrad.* **1**, 117–126 (1993).
20. Tokiwa, Y., Calabia, B. P., Ugwu, C. U. & Aiba, S. Biodegradability of plastics. *Int. J. Mol. Sci.* **10**, 3722–3742 (2009).
21. Thompson, R. C. *et al.* Lost at Sea: Where Is All the Plastic? *Science (80-.).* **304**, 838 (2004).
22. Hidalgo-Ruz, V., Gutow, L., Thompson, R. C. & Thiel, M. Microplastics in the marine environment: A review of the methods used for identification and quantification. *Environ. Sci. Technol.* **46**, 3060–3075 (2012).
23. Arthur, C., Baker, J. & Bamford, H. Proceedings of the International Research Workshop on the Occurrence , Effects , and Fate of Microplastic Marine Debris. *Group* 530 (2009).
24. Picó, Y. & Barceló, D. Analysis and prevention of microplastics pollution in water: Current perspectives and future directions. *ACS Omega* **4**, 6709–6719 (2019).
25. Oceanic, N. Laboratory Methods for the Analysis of Microplastics in the Marine Environment : Recommendations for quantifying synthetic particles in waters and sediments. (2015).
26. European commission. Plastic waste: ecological and human health impacts. *Sci. Environ. Policy* 1–37 (2011) doi:KH-31-13-768-EN-N.
27. Alimi, O. S., Farner Budarz, J., Hernandez, L. M. & Tufenkji, N. Microplastics and Nanoplastics in Aquatic Environments: Aggregation, Deposition, and Enhanced Contaminant Transport. *Environ. Sci. Technol.* **52**, 1704–1724 (2018).
28. Rios Mendoza, L. M. & Balcer, M. Microplastics in freshwater environments: A review of quantification assessment. *TrAC - Trends Anal. Chem.* **113**, 402–408 (2019).
29. Hartmann, N. B. *et al.* Are We Speaking the Same Language? Recommendations for a Definition and Categorization Framework for Plastic Debris. *Environ. Sci. Technol.* **53**, 1039–1047 (2019).
30. Auffan, M. *et al.* Towards a definition of inorganic nanoparticles from an environmental, health and safety perspective. *Nat. Nanotechnol.* **4**, 634–641 (2009).
31. Gigault, J. *et al.* Current opinion: What is a nanoplastic? *Environ. Pollut.* **235**, 1030–1034 (2018).
32. Schwaferts, C., Niessner, R., Elsner, M. & Ivleva, N. P. Methods for the analysis of submicrometer- and nanoplastic particles in the environment. *TrAC - Trends Anal. Chem.* **112**, 52–65 (2019).
33. Schwarz, A. E., Ligthart, T. N., Boukris, E. & van Harmelen, T. Sources, transport, and accumulation of different types of plastic litter in aquatic environments: A review study. *Mar. Pollut. Bull.* **143**, 92–100 (2019).
34. Zbyszewski, M., Corcoran, P. L. & Hockin, A. Comparison of the distribution and degradation of plastic debris along shorelines of the Great Lakes, North America. *J. Great Lakes Res.* **40**, 288–299 (2014).

35. Nguyen, B. *et al.* Separation and Analysis of Microplastics and Nanoplastics in Complex Environmental Samples. *Acc. Chem. Res.* **52**, 858–866 (2019).
36. Ekvall, M. T. *et al.* Nanoplastics formed during the mechanical breakdown of daily-use polystyrene products. *Nanoscale Adv.* **1**, 1055–1061 (2019).
37. L. Sheng, M. Christopher, A. M. Toxicological considerations of nano-sized particles. *Physiol. Behav.* **176**, 100–106 (2019).
38. Bouwmeester, H., Hollman, P. C. H. & Peters, R. J. B. Potential Health Impact of Environmentally Released Micro- and Nanoplastics in the Human Food Production Chain: Experiences from Nanotoxicology. *Environ. Sci. Technol.* **49**, 8932–8947 (2015).
39. Reano, A. F., Guinault, A., Richaud, E. & Fayolle, B. Polyethylene loss of ductility during oxidation: Effect of initial molar mass distribution. *Polym. Degrad. Stab.* **149**, 78–84 (2018).
40. El Hadri, H., Gigault, J., Maxit, B., Grassl, B. & Reynaud, S. Nanoplastic from mechanically degraded primary and secondary microplastics for environmental assessments. *NanoImpact* **17**, 100206 (2020).
41. Nanoplastic should be better understood. *Nat. Nanotechnol.* **14**, 299 (2019).
42. Wagner, S. & Reemtsma, T. Things we know and don't know about nanoplastic in the environment. *Nat. Nanotechnol.* **14**, 300–301 (2019).
43. Kögel, T., Bjorøy, Ø., Toto, B., Bienfait, A. M. & Sanden, M. Micro- and nanoplastic toxicity on aquatic life: Determining factors. *Sci. Total Environ.* **709**, 136050 (2020).
44. Wright, S. L. & Kelly, F. J. Plastic and Human Health: A Micro Issue? *Environ. Sci. Technol.* **51**, 6634–6647 (2017).
45. Jovanović, B. Ingestion of microplastics by fish and its potential consequences from a physical perspective. *Integr. Environ. Assess. Manag.* **13**, 510–515 (2017).
46. Sussarellu, R. *et al.* Oyster reproduction is affected by exposure to polystyrene microplastics. *Proc. Natl. Acad. Sci. U. S. A.* **113**, 2430–2435 (2016).
47. Barboza, L. G. A. *et al.* Microplastics in wild fish from North East Atlantic Ocean and its potential for causing neurotoxic effects, lipid oxidative damage, and human health risks associated with ingestion exposure. *Sci. Total Environ.* **717**, 134625 (2020).
48. *et al.* Microplastics in urban New Jersey freshwaters: distribution, chemical identification, and biological affects. *AIMS Environ. Sci.* **4**, 809–826 (2017).
49. Rochman, C. M., Hentschel, B. T. & The, S. J. Long-term sorption of metals is similar among plastic types: Implications for plastic debris in aquatic environments. *PLoS One* **9**, (2014).
50. Manabe, M., Tatarazako, N. & Kinoshita, M. Uptake, excretion and toxicity of nano-sized latex particles on medaka (Oryzias latipes) embryos and larvae. *Aquat. Toxicol.* **105**, 576–581 (2011).
51. Karami, A., Romano, N., Galloway, T. & Hamzah, H. Virgin microplastics cause toxicity and modulate the impacts of phenanthrene on biomarker responses in African catfish (Clarias gariepinus). *Environ. Res.* **151**, 58–70 (2016).
52. Cedervall, T., Hansson, L. A., Lard, M., Frohm, B. & Linse, S. Food chain transport of nanoparticles affects behaviour and fat metabolism in fish. *PLoS One* **7**, 1–6 (2012).

53. Chen, Q. *et al.* Quantitative investigation of the mechanisms of microplastics and nanoplastics toward zebrafish larvae locomotor activity. *Sci. Total Environ.* **584–585**, 1022–1031 (2017).
54. Jin, Y. *et al.* Polystyrene microplastics induce microbiota dysbiosis and inflammation in the gut of adult zebrafish. *Environ. Pollut.* **235**, 322–329 (2018).
55. Brown, D. M., Wilson, M. R., MacNee, W., Stone, V. & Donaldson, K. Size-dependent proinflammatory effects of ultrafine polystyrene particles: A role for surface area and oxidative stress in the enhanced activity of ultrafines. *Toxicol. Appl. Pharmacol.* **175**, 191–199 (2001).
56. Heddagaard, F. E. & Møller, P. Hazard assessment of small-size plastic particles: is the conceptual framework of particle toxicology useful? *Food Chem. Toxicol.* **136**, 111106 (2020).
57. Cox, K. D. *et al.* Human Consumption of Microplastics. *Environ. Sci. Technol.* **53**, 7068–7074 (2019).
58. Barboza, L. G. A., Dick Vethaak, A., Lavorante, B. R. B. O., Lundebye, A. K. & Guilhermino, L. Marine microplastic debris: An emerging issue for food security, food safety and human health. *Mar. Pollut. Bull.* **133**, 336–348 (2018).
59. Presence of microplastics and nanoplastics in food, with particular focus on seafood. *EFSA J.* **14**, (2016).
60. Lehner, R., Weder, C., Petri-Fink, A. & Rothen-Rutishauser, B. Emergence of Nanoplastic in the Environment and Possible Impact on Human Health. *Environ. Sci. Technol.* (2019) doi:10.1021/acs.est.8b05512.
61. Silva, A. B. *et al.* Microplastics in the environment: Challenges in analytical chemistry - A review. *Anal. Chim. Acta* **1017**, 1–19 (2018).
62. Rochman, C. M., Regan, F. & Thompson, R. C. On the harmonization of methods for measuring the occurrence, fate and effects of microplastics. *Anal. Methods* **9**, 1324–1325 (2017).
63. Karlsson, T. M., Kärrman, A., Rotander, A. & Hassellöv, M. Comparison between manta trawl and in situ pump filtration methods, and guidance for visual identification of microplastics in surface waters. *Environ. Sci. Pollut. Res.* **27**, 5559–5571 (2020).
64. Wang, W. & Wang, J. Investigation of microplastics in aquatic environments: An overview of the methods used, from field sampling to laboratory analysis. *TrAC - Trends Anal. Chem.* **108**, 195–202 (2018).
65. Bishop, J. K. B., Lam, P. J. & Wood, T. J. Getting good particles: Accurate sampling of particles by large volume in-situ filtration. *Limnol. Oceanogr. Methods* **10**, 681–710 (2012).
66. Chen, Y. J. *et al.* Application of fenton method for the removal of organic matter in sewage sludge at room temperature. *Sustain.* **12**, 1–10 (2020).
67. Tagg, A. S. *et al.* Fenton's reagent for the rapid and efficient isolation of microplastics from wastewater. *Chem. Commun.* **53**, 372–375 (2017).
68. Imhof, H. K., Schmid, J., Niessner, R., Ivleva, N. P. & Laforsch, C. A novel, highly efficient method for the separation and quantification of plastic particles in sediments of aquatic environments. *Limnol. Oceanogr. Methods* **10**, 524–537 (2012).
69. Foekema, E. M. *et al.* Plastic in north sea fish. *Environ. Sci. Technol.* **47**, 8818–

8824 (2013).
70. Al-azzawi, M. S. M. *et al.* Validation of Sample Preparation Methods for Microplastic Analysis in Wastewater. *Water* **12**, 2445 (2020).
71. Löder, M. G. J. *et al.* Enzymatic Purification of Microplastics in Environmental Samples. *Environ. Sci. Technol.* **51**, 14283–14292 (2017).
72. Nuelle, M. T., Dekiff, J. H., Remy, D. & Fries, E. A new analytical approach for monitoring microplastics in marine sediments. *Environ. Pollut.* **184**, 161–169 (2014).
73. Renner, G., Schmidt, T. C. & Schram, J. Analytical methodologies for monitoring micro(nano)plastics: Which are fit for purpose? *Curr. Opin. Environ. Sci. Heal.* **1**, 55–61 (2018).
74. Huppertsberg, S. & Knepper, T. P. Validation of an FT-IR microscopy method for the determination of microplastic particles in surface waters. *MethodsX* **7**, (2020).
75. Zobkov, M. B. & Esiukova, E. E. Microplastics in a Marine Environment: Review of Methods for Sampling, Processing, and Analyzing Microplastics in Water, Bottom Sediments, and Coastal Deposits. *Oceanology* **58**, 137–143 (2018).
76. Lusher, A. L., Bråte, I. L. N., Munno, K., Hurley, R. R. & Welden, N. A. Is It or Isn't It: The Importance of Visual Classification in Microplastic Characterization. *Appl. Spectrosc.* **74**, 1139–1153 (2020).
77. Maes, T., Jessop, R., Wellner, N., Haupt, K. & Mayes, A. G. A rapid-screening approach to detect and quantify microplastics based on fluorescent tagging with Nile Red. *Sci. Rep.* **7**, 1–10 (2017).
78. Fischer, E. K., Paglialonga, L., Czech, E. & Tamminga, M. Microplastic pollution in lakes and lake shoreline sediments - A case study on Lake Bolsena and Lake Chiusi (central Italy). *Environ. Pollut.* **213**, 648–657 (2016).
79. Li, J. *et al.* Microplastics in mussels along the coastal waters of China. *Environ. Pollut.* **214**, 177–184 (2016).
80. Nguyen, B. *et al.* Separation and Analysis of Microplastics and Nanoplastics in Complex Environmental Samples. *Acc. Chem. Res.* **52**, 858–866 (2019).
81. Fries, E. *et al.* Identification of polymer types and additives in marine microplastic particles using pyrolysis-GC/MS and scanning electron microscopy. *Environ. Sci. Process. Impacts* **15**, 1949–1956 (2013).
82. Dümichen, E. *et al.* Analysis of polyethylene microplastics in environmental samples, using a thermal decomposition method. *Water Res.* **85**, 451–457 (2015).
83. Xu, J. L., Thomas, K. V., Luo, Z. & Gowen, A. A. FTIR and Raman imaging for microplastics analysis: State of the art, challenges and prospects. *TrAC - Trends Anal. Chem.* **119**, 115629 (2019).
84. Shim, W. J., Hong, S. H. & Eo, S. E. Identification methods in microplastic analysis: A review. *Anal. Methods* **9**, 1384–1391 (2017).
85. Harrison, J. P., Ojeda, J. J. & Romero-González, M. E. The applicability of reflectance micro-Fourier-transform infrared spectroscopy for the detection of synthetic microplastics in marine sediments. *Sci. Total Environ.* **416**, 455–463 (2012).
86. Vianello, A. *et al.* Microplastic particles in sediments of Lagoon of Venice, Italy: First observations on occurrence, spatial patterns and identification. *Estuar. Coast. Shelf Sci.* **130**, 54–61 (2013).

87. Primpke, S., Lorenz, C., Rascher-Friesenhausen, R. & Gerdts, G. An automated approach for microplastics analysis using focal plane array (FPA) FTIR microscopy and image analysis. *Anal. Methods* **9**, 1499–1511 (2017).
88. Driedger, A. G. J., Dürr, H. H., Mitchell, K. & Van Cappellen, P. Plastic debris in the Laurentian Great Lakes: A review. *J. Great Lakes Res.* **41**, 9–19 (2015).
89. Hendrickson, E., Minor, E. C. & Schreiner, K. Microplastic abundance and composition in western Lake Superior as determined via microscopy, Pyr-GC/MS, and FTIR. *Environ. Sci. Technol.* **52**, 1787–1796 (2018).
90. Dris, R., Gasperi, J., Saad, M., Mirande, C. & Tassin, B. Synthetic fibers in atmospheric fallout: A source of microplastics in the environment? *Mar. Pollut. Bull.* **104**, 290–293 (2016).
91. Browne, M. A. *et al.* Accumulation of microplastic on shorelines woldwide: Sources and sinks. *Environ. Sci. Technol.* **45**, 9175–9179 (2011).
92. Zbyszewski, M. & Corcoran, P. L. Distribution and degradation of fresh water plastic particles along the beaches of Lake Huron, Canada. *Water. Air. Soil Pollut.* **220**, 365–372 (2011).
93. Summary of Pellet Clean-Up Activities. *Canadian Pacific* (May 2016).
94. Sterner, R. W. *et al.* Ecosystem services of Earth's largest freshwater lakes. *Ecosyst. Serv.* **41**, 101046 (2020).
95. Bergmann, M., Mützel, S., Primpke, S. & Tekman, M. B. White and wonderful ? Microplastics prevail in snow from the Alps to the Arctic. 1–11 (2019).
96. Hebner, T. S. & Maurer-Jones, M. A. Characterizing microplastic size and morphology of photodegraded polymers placed in simulated moving water conditions. *Environ. Sci. Process. Impacts* **22**, 398–407 (2020).
97. Baldwin, A. K., Corsi, S. R. & Mason, S. A. Plastic Debris in 29 Great Lakes Tributaries: Relations to Watershed Attributes and Hydrology. *Environ. Sci. Technol.* **50**, 10377–10385 (2016).
98. Lenaker, P. L., Corsi, S. R. & Mason, S. A. Spatial Distribution of Microplastics in Surficial Benthic Sediment of Lake Michigan and Lake Erie. *Environ. Sci. Technol.* **55**, 373–384 (2021).
99. Corcoran, P. L. *et al.* Hidden plastics of Lake Ontario, Canada and their potential preservation in the sediment record. *Environ. Pollut.* **204**, 17–25 (2015).
100. Grbić, J., Helm, P., Athey, S. & Rochman, C. M. Microplastics entering northwestern Lake Ontario are diverse and linked to urban sources. *Water Res.* **174**, (2020).
101. Lenaker, P. L. *et al.* Vertical Distribution of Microplastics in the Water Column and Surficial Sediment from the Milwaukee River Basin to Lake Michigan. *Environ. Sci. Technol.* **53**, 12227–12237 (2019).
102. Morét-Ferguson, S. *et al.* The size, mass, and composition of plastic debris in the western North Atlantic Ocean. *Mar. Pollut. Bull.* **60**, 1873–1878 (2010).
103. Chamas, A. *et al.* Degradation Rates of Plastics in the Environment. *ACS Sustain. Chem. Eng.* **8**, 3494–3511 (2020).
104. Fazey, F. M. C. & Ryan, P. G. Biofouling on buoyant marine plastics: An experimental study into the effect of size on surface longevity. *Environ. Pollut.* **210**, 354–360 (2016).
105. Whitaker, J. M., Garza, T. N. & Janosik, A. M. Sampling with Niskin bottles and

microfiltration reveals a high prevalence of microfibers. *Limnologica* **78**, (2019).
106. Tekman, M. B. *et al.* Tying up Loose Ends of Microplastic Pollution in the Arctic: Distribution from the Sea Surface through the Water Column to Deep-Sea Sediments at the HAUSGARTEN Observatory. *Environ. Sci. Technol.* **54**, 4079–4090 (2020).
107. Claessens, M., Meester, S. De, Landuyt, L. Van, Clerck, K. De & Janssen, C. R. Occurrence and distribution of microplastics in marine sediments along the Belgian coast. *Mar. Pollut. Bull.* **62**, 2199–2204 (2011).
108. Minor, E. C., Tennant, C. J. & Brown, E. T. A Seasonal to Interannual View of Inorganic and Organic Carbon and pH in Western Lake Superior. *J. Geophys. Res. Biogeosciences* **124**, 405–419 (2019).
109. Martin, K. M., Hasenmueller, E. A., White, J. R., Chambers, L. G. & Conkle, J. L. Sampling, sorting, and characterizing microplastics in aquatic environments with high suspended sediment loads and large floating debris. *J. Vis. Exp.* **2018**, 1–9 (2018).
110. Jung, M. R. *et al.* Validation of ATR FT-IR to identify polymers of plastic marine debris, including those ingested by marine organisms. *Mar. Pollut. Bull.* **127**, 704–716 (2018).
111. Gago, J., Galgani, F., Maes, T. & Thompson, R. C. Microplastics in seawater: Recommendations from the marine strategy framework directive implementation process. *Front. Mar. Sci.* **3**, (2016).
112. Vega-Moreno, D. *et al.* Distribution and transport of microplastics in the upper 1150 m of the water column at the Eastern North Atlantic Subtropical Gyre, Canary Islands, Spain. *Sci. Total Environ.* **788**, 147802 (2021).
113. Olesen, K. B., Alst, N. Van, Simon, M. & Vianello, A. Analysis of Microplastics using FTIR Imaging Identifying and quantifying microplastics in. (2017).
114. Lorenzo-Navarro, J., Castrillón-Santana, M., Gómez, M., Herrera, A. & Marín-Reyes, P. A. Automatic counting and classification of microplastic particles. *ICPRAM 2018 - Proc. 7th Int. Conf. Pattern Recognit. Appl. Methods* **2018-January**, 646–652 (2018).

APPENDICES

Appendix A

To test the recovery of microplastics with the filter tower, a known quantity of microplastics (Table 8) was added and mixed with 10 liters of Milli-Q water in a 10-liter carboy. This spiked water was then slowly poured into the top of the filter tower. The filter tower was fitted with 300 µm, 100 µm, 50 µm, and 5 µm nylon mesh filters as it was in the field. Once all the water was filtered, the carboy was rinsed with Milli-Q water and this rinsate was also poured into the filter tower. Before removal of each filter with clean metal forceps, the interior circumference of the filter tower above each filter was rinsed with Milli-Q water to ensure all plastic particles were washed onto the filters. The filters were removed from the top such that first the 300 µm filter was removed, then the 100 µm, then the 50 µm, and lastly the 5 µm at the very bottom of the tower.

Table 8. Filter tower test plastics.

Plastic Type	**Size (µm)**	**Weight (mg)**
Polyethylene (PE)	350	16.409
Polyvinylchloride (PVC)	250	16.205
Polyethylene (PE)	10-45	16.627
		Total: 49.241

Each filter was then thoroughly rinsed into a pre-weighed 250 ml glass beaker with Milli-Q water to remove all plastic particles. These beakers were then placed in an oven at 90°C to evaporate the water. After evaporation, the beakers were taken from the oven and allowed to equilibrate to the ambient temperature and humidity. The beakers were then weighed, and the overall percent recovery was determined (Table 9). The percent recovery for each filter was also determined based on which filter we would expect the various size microplastic standards to be captured.

Table 9. Filter tower testing results.

Filter	Expected wt. (mg)	Recovered wt. (mg)	% Recovery
300 µm	16.409	21.50	131.0
100 µm	16.205	14.40	88.9
50 µm	0.0	2.70	-
5 µm	16.627	10.30	61.9
Total	49.241	48.9	99.3

During initial recovery testing from the filter tower (results not reported here), the filters were thoroughly rinsed with Milli-Q water into pre-weighed aluminum pans before evaporation at 90°C in the oven. However, these hot and humid conditions visibly oxidized the aluminum pans, adding weight to them so that it was not possible to obtain an accurate recovered weight. Ultimately, it was decided that accurate recoveries could only be obtained if evaporations were carried out in glass beakers. During initial testing of microplastic recovery protocols, evaporation via hotplate heating was also attempted. This technique, however, was not as reliable as evaporation at 90°C in the oven and was prone to melting and burning the microplastics. Therefore, hotplate evaporations were abandoned in favor of oven evaporation (as performed for the samples in Table 9).

Appendix B

To test the recovery of microplastics with the filtration manifold attached to the pressurized 20-liter Cornelius kegs, a known quantity of microplastics (Table 10) was added and mixed with 20 liters of deionized water in one Cornelius keg. The keg was then pressurized and the water within was filtered through a cascade of 47 mm diameter 100 µm, 50 µm, and 5 µm nylon mesh filters placed within the filtration manifold. Once all the water was filtered, the keg was depressurized, and the interior was rinsed with Milli-Q water such that all particles clinging to the interior of the keg were rinsed down to the sump at the bottom of the keg. The keg was again pressurized and the rinsate in the sump was filtered through the filtration manifold. The manifold was then disassembled, and each filter was extracted from its stainless-steel housing using clean metal forceps. Each filter was then carefully rinsed with Milli-Q water into the same pre-weighed beaker. This beaker was then placed in an oven at 90°C to evaporate the water. After evaporation, the beaker was taken from the oven and allowed to equilibrate to the ambient temperature and humidity. The beaker was then weighed, and the percent recovery was determined. 39.8 mg of the original 47.7 mg of microplastics were recovered through this technique, a recovery percent of 83.5%. Accordingly, it will be necessary to multiply the number of particles captured by this sampling technique by a factor of approximately 1.19 to account for this recovery discrepancy.

Table 10. Filtration manifold test plastics.

Plastic Type	**Size (µm)**	**Weight (mg)**
Polyvinylchloride (PVC)	250	15.113
Polystyrene (PS)	250	16.438
Polyethylene (PE)	10-45	16.138
		Total: 47.689